
Supporting Information:

Lipid head group parameterisation for GROMOS 54a8: a consistent approach with
protein force field description

Irene Marzuoli, Christian Margreitter and Franca Fraternali

Randall Centre for Cell and Molecular Biology, King's College London, London

List of Tables

1	Table of additional control simulations	7
2	Table of simulations for POPE bilayer	7
3	Table of compressibility values for PC lipids	8
4	Table of thickness values for PC lipids	8
5	Table of water molecules per lipid moiety for PC lipids	9
6	Table of computed properties of POPE bilayer	10
7	Table of water molecules per lipid moiety for POPE bilayer	10
8	Table of computed properties of POPG bilayer	10
9	Table of water molecules per lipid moiety for POPG bilayer	10
10	Comparison with previous parameters and simulations setup	11

List of Figures

1	Dipole potential	4
2	Time series of the area per lipid for a DPPC bilayer	12
3	Comparison of Area per Lipid for different time windows of the same simulation	13
4	Area per lipid for control simulations	14
5	Comparison of key properties across parameter sets for a DLPC bilayer	15
6	Comparison of key properties across parameter sets for a DMPC bilayer	16
7	Comparison of key properties across parameter sets for a DOPC bilayer	17
8	Comparison of key properties across parameter sets for a POPC bilayer	18
9	Comparison of key properties across parameter sets for a DPPC bilayer	19
10	Electron density profiles of bilayers for parameter set Chiu/54A7	20
11	Electron density profiles of bilayers for parameter set Chiu/54A8	21
12	Electron density profiles of bilayers for parameter set RM/54A8_v2	22
13	Electron density profiles of bilayers for parameter set RM/54A8_v3	23
14	Deuterium order parameter S_{CD} of bilayers for parameter set Chiu/54A8 . .	24
15	Deuterium order parameter S_{CD} of bilayers for parameter set RM/54A8_v2 .	25
16	Deuterium order parameter S_{CD} of bilayers for parameter set RM/54A8_v3 .	26
17	Hydration profiles for DLPC bilayer across parameter sets	27
18	Hydration profiles for DMPC bilayer across parameter sets	28
19	Hydration profiles for DOPC bilayer across parameter sets	29
20	Hydration profiles for POPC bilayer across parameter sets	30
21	Phosphocholine moieties SASA	31
22	Head group orientation, lipid tails comparison	32
23	Head group orientation, parameter sets comparison	33
24	Diffusion coefficient of DPPC in control simulations	34
25	Snapshot of DPPC patch partially in gel phase	35
26	Key properties of POPE bilayer for parameter set Chiu/54A8/CH0	36
27	Key properties of POPE bilayer for parameter set RM/54A8/CH0	37

28	Key properties of POPG bilayer for parameter set RM/54A8/CH0	38
29	Scheme of the 1LFC orientations chosen for the peptide-membrane simulations	39
30	1LFC orientation with respect to membrane plane along simulations	40

1 Supplementary results: dipole potential

For the five phospholipids and the five different parameters tested, we computed the dipole potential across the membrane, according to the procedure outlined in Section 2.5 of the paper.

The results are outlined in Figure 1 and show a striking difference between the profiles obtained with the Chiu partial charges set and the Reif-Margreitter one: in particular, while the former suggests local maxima of the dipole potential in the head regions, the latter results in a potential rising to its higher value in the center of the tails region.

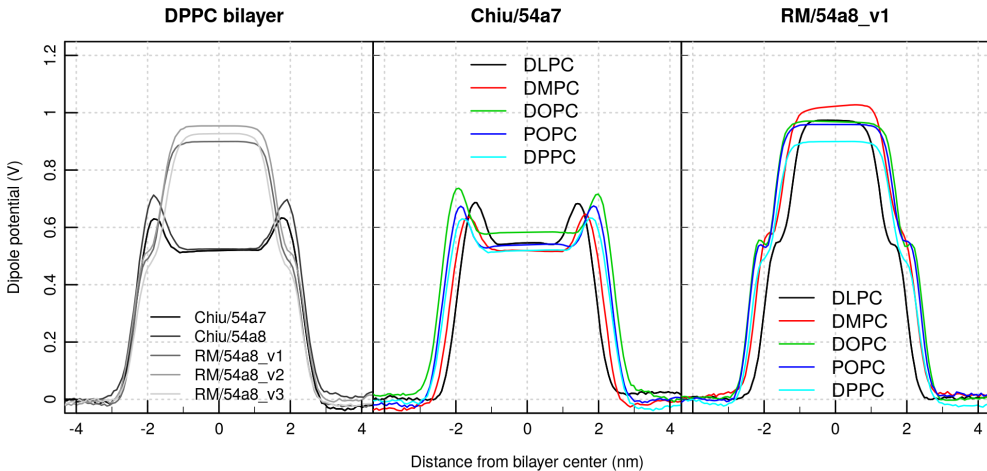


Figure 1: Dipole potential for respectively: (left) a DPPC bilayer, simulated with the five parameter sets explored in the manuscript; (center) the five different phospholipid considered and parameter set Chiu/54a7; (right) the five different phospholipid considered and parameter set RM/54a8_v1.

The results for the Chiu set of partial charges (and either the 54a7 or 54a8 GROMOS force field) are compatible with what obtained previously by Gurtovenko et al. in Ref. [7] using the same charges and the Berger force field (a slight modification of GROMOS tailored for lipids simulations). On the contrary, the new results are qualitatively more similar to what obtained with the all atom force field CHARMM36 in Ref. [4] and [23], as they both suggest a peak of the potential in the lipid tail regions. However, with respect to the CHARMM36 profiles, the ones obtained by the RM/54a8_v1 parameters give a flatter trend in the center

of the bilayer. Moreover, the peaks relative to the phosphate regions are shallower for the RM/54a8_v1 simulations with respect to the CHARMM ones.

To discriminate between the two behaviours it is necessary a comparison with experimental results. Few works compute the profile of the dipole potential along the bilayer normal, focussing instead on measuring the difference between the dipole potential on the two sides of the bilayer [20, 19, 13]. Never the less, Wang et al. [22] measured its profile for ester-DPhPC lipid vesicles, suggesting a peak in the central region of the bilayer. This lipid is derived from DPPC by adding an ester linkage: as such, its profile will not be identical to the one produced by DPPC, but being the modification in the ester region only, we can assume that the qualitative trend remains the same and thus can be used for the present comparison.

Additionally to experimental data, theoretical profiles obtained from ab initio calculations and geometrical assumptions on the structure of lipids bilayers suggest indeed a plateau in the tail region [3] - or at the very least do not support the presence of peaks in the head regions, as showed when the Chiu charge set is used in the simulations.

For all the above reasons we once more consider the new set of parameter (RM/54a8_v1) as a better compromise than the previous sets Chiu/54a7 or Chiu/54a8.

Supplementary Movie 1: file LFC_54a8_v1_0.mp4

The movie displays the simulation of LFC on a bacterial membrane (composition DLPC:DLPG with 3:1 ratio) for both parameter set Chiu/54a8 (left half) and RM/54a8_v1 (right half), starting from orientation OII. The lipid choline and phosphate atoms are shown as van der Waals beads, the protein as cyan cartoon and bonds coloured by residue type (blue positive, green polar, white hydrophobic) except for the two Tryptophan residues which are coloured in orange.

Control simulations

Sim	Charges ^a	FF	Long range ES ^b	Nr lipids	T (K)
0	RM	54A7	PME	512	323
RF	Chiu	54A7	RF	512	323
Small	Chiu	54A7	PME	128	323
303	RM	54A8_v1	PME	512	303
333	RM	54A8_v1	PME	512	333

Table 1: Table of additional control simulations, run on the DPPC bilayer. ^a Charge set: Chiu from Ref [2], RM Reif-Margreitter as illustrated in the present work. ^b RF reaction field [21], PME Particle Mesh Ewald summation [6].

Simulations of POPE

Sim	Charges ^a	FF	Ester carbon type
1CH0	PC	54a8	CH0
CH0	RM	54a8	CH0

Table 2: Table of simulations for POPE. All are run for 500 ns and systems consisting of 512 lipid molecules (256 per layer), using a PME long range electrostatic scheme. ^a Charge set: PC Piggot-Chiu from Ref [14], RM Reif-Margreitter as illustrated in the present work.

K_A (mN m^{-1})						
ID	Charges/FF	DLPC	DMPC	DOPC	POPC	DPPC
1	Chiu/54A7	553	477	607	515	499
2	Chiu/54a8	471	500	471	679	612
3	RM/54a8_v1	562	354	485	397	329
4	RM/54a8_v2	365	318	518	466	406
5	RM/54a8_v3	332	300	426	345	376
Experiment ^a		234(23)	188-265(18)	231(20)	180-330	248(20)

Table 3: Average isothermal area compressibility module K_A over the last 300 ns of simulations for phosphocholine bilayers. All simulations run at 303 K, except for DPPC (323 K). ^a Values from Ref. [9] and Table 1 in Ref. [15], in parenthesis the standard error on the last digit is shown.

Hydrophobic thickness D_{HH} (nm)						
ID	Charges/FF	DLPC	DMPC	DOPC	POPC	DPPC
1	Chiu/54A7	2.83	3.59	3.05	3.30	4.30
2	Chiu/54a8	2.78	3.52	2.90	3.14	4.21
3	RM/54a8_v1	2.72	3.48	2.89	3.22	4.06
4	RM/54a8_v2	2.61	3.33	2.82	3.08	4.06
5	RM/54a8_v3	2.38	3.13	2.65	2.86	3.77
Experiment ^a		3.08	3.44-3.60	3.53-3.71	3.70	3.42-3.83
Luzzati thickness D_B (nm)						
ID	Charges/FF	DLPC	DMPC	DOPC	POPC	DPPC
1	Chiu/54A7	3.11	3.54	4.13	4.00	3.93
2	Chiu/54a8	3.14	3.61	3.97	3.96	3.96
3	RM/54a8_v1	3.04	3.48	3.94	3.88	3.75
4	RM/54a8_v2	3.00	3.34	3.87	3.77	3.74
5	RM/54a8_v3	2.80	3.21	3.62	3.57	3.50
Experiment ^a		3.14	3.63-3.96	3.59-3.87	3.68	3.50-3.83

Table 4: Bilayer thickness, according to the Phosphate or Luzzati methods, derived from the electron density profiles of phosphocholine bilayers. All simulations run at 303 K, except for DPPC (323 K). ^a Values from Ref. [16] and Table 1 in Ref. [15]

		Nr water molecules per group				
Group	ID	DLPC	DMPC	DOPC	DPPC	POPC
All	1	3.9 (13.2)	3.8 (12.9)	3.9 (13.3)	3.7 (12.7)	3.8 (13.1)
	2	3.6 (12.7)	3.5 (12.4)	3.6 (12.9)	3.4 (12.3)	3.6 (12.6)
	3	4.3 (14.1)	4.3 (13.8)	4.4 (14.3)	4.2 (13.7)	4.3 (14.1)
	4	4.6 (15.1)	4.6 (15.0)	4.6 (15.1)	4.5 (14.7)	4.6 (15.1)
	5	5.1 (16.9)	5.1 (16.8)	5.0 (16.9)	4.9 (16.6)	5.1 (16.8)
Cho	1	13.1	12.8	13.3	12.6	13.1
	2	12.6	12.3	12.7	12.2	12.5
	3	14.3	14.1	14.5	13.9	14.3
	4	15.3	15.2	15.4	14.9	15.3
	5	17.0	16.9	17.0	16.7	17.0
PO4	1	3.1 (9.8)	3.0 (9.6)	3.1 (9.9)	3.1 (9.6)	3.1 (9.8)
	2	2.6 (9.3)	2.5 (9.0)	2.6 (9.4)	2.6 (9.2)	2.5 (9.2)
	3	4.0 (9.8)	4.0 (9.6)	4.0 (9.9)	3.9 (9.8)	4.0 (9.8)
	4	4.3 (10.3)	4.3 (10.3)	4.3 (10.4)	4.2 (10.3)	4.3 (10.4)
	5	4.8 (11.5)	4.7 (11.5)	4.8 (11.5)	4.7 (11.5)	4.8 (11.5)
Gly	1	0.3 (3.5)	0.3 (3.4)	0.3 (3.5)	0.3 (3.4)	0.3 (3.5)
	2	0.3 (3.4)	0.2 (3.2)	0.3 (3.4)	0.2 (3.3)	0.2 (3.3)
	3	0 (3.5)	0 (3.5)	0 (3.6)	0 (3.4)	0 (3.5)
	4	0 (3.8)	0 (3.8)	0 (3.8)	0 (3.7)	0 (3.8)
	5	0 (4.3)	0 (4.3)	0 (4.2)	0 (4.2)	0 (4.3)
CO1	1	1.4	1.4	1.4	1.4	1.4
	2	1.5	1.5	1.5	1.5	1.5
	3	1.2	1.2	1.2	1.1	1.2
	4	1.3	1.2	1.3	1.1	1.3
	5	1.3	1.3	1.3	1.3	1.3
CO2	1	0.5	0.5	0.5	0.5	0.5
	2	0.6	0.6	0.6	0.6	0.6
	3	0.7	0.6	0.7	0.6	0.7
	4	0.7	0.7	0.7	0.7	0.7
	5	0.8	0.8	0.8	0.8	0.8

Table 5: Integrated value of water molecules around each lipid and for their constituting chemical groups (Cho: choline, PO4: phosphate, Gly: glycerol, CO1 and CO2: carbonyl groups at the sn-1 and sn-2 positions). The integration is performed up to the first peak and, if applicable, to the second (the latter of which is given in brackets). Peak positions are the same throughout the simulations, except for glycerol in ID3 to ID5, where the first peak is not shown (thus the value of 0, see main text for interpretation).

POPE (313 K) structural properties

ID	Charges/FF/ester	ApL (nm ²)	K _A (mN m ⁻¹)	D _{HH} (nm)	D _B (nm)
1CH0	Chiu/54a8/CH0	0.591(5)	437	2.48	3.92
CH0	RM/54a8/CH0	0.595(5)	361	2.52	3.89
Experiment ^a		0.566	—	—	4.13

Table 6: Area per lipid, lateral compressibility and bilayer thickness, according to the phosphate or Luzzati methods, derived from the electron density profiles for POPE bilayer. ^a From [17].

POPE (313 K) Nr water molecules per group

ID	Charges/FF/ester	All	Am	PO4	Gly	CO1	CO2
1CH0	Chiu/54a8/CH0	1.6 (5.7)	2.2	3.3 (10.6)	0 (3.4)	0.8	0.5
CH0	RM/54a8/CH0	2.1 (6.4)	2.5	4.2 (11.3)	0 (3.6)	0.6	0.6

Table 7: Number of water molecules per lipid hydrating the POPE bilayer and its different polar moieties (Am: amine, PO4: phosphate, Gly: glycerol, CO1 and CO2: carbonyl groups at the sn-1 and sn-2 positions). Integration was performed up to the first peak and when relevant to the second one (value in bracket). Peak positions are the same for both simulations.

POPG (303 K) structural properties

ID	Charges/FF/ester	ApL (nm ²)	K _A (mN m ⁻¹)	D _{HH} (nm)	D _B (nm)
CH0	RM/54a8/CH0	0.646(7)	198	3.76	3.98
Experiment ^a		0.661(13)	—	3.74(7)	—

Table 8: Area per lipid, lateral compressibility and bilayer thickness, according to the phosphate or Luzzati methods, derived from the electron density profiles. ^a From [11].

POPG (303 K) Nr water molecules per group

ID	Charges/FF/ester	All	Etam	PO4	Gly	CO1	CO2
H0	RM/54a8/CH0	0.2 (3.7)	0.5 (7.8)	3.9	3.2 (6.2)	0.5	0.4

Table 9: Number of water molecules per lipid hydrating the POPG bilayer and its different polar moieties (Etam: etamine, PO4: phosphate, Gly: glycerol, CO1 and CO2: carbonyl groups at the sn-1 and sn-2 positions). Integration was performed up to the first peak, and when relevant to the second one (value in bracket). Peak positions are the same for both simulations.

Comparison with the previous parameterization work

	Poger et al. [16, 15]	Present work	
Lipid parameters			
Choline partial charges	Chiu [2]	Reif	[18]
Phosphate partial charges	Chiu [2]	Margreitter	[8]
CH3p-OM C12 [$\text{kJ mol}^{-1}\text{nm}^{12}$]	$1.58E-5$ [16]	$1.10E-5$	Present work
CH3p-CH3p C12 [$\text{kJ mol}^{-1}\text{nm}^{12}$]	$2.66E-5$ [10]	$6.48E-5$	[18]
Simulations details			
GROMACS version	3.2.1	2016.3	[1]
Long range electrostatics	Reaction Field [21]	PME	[6]
Cut-off ^a	Twin-range	Single	
Short range cut-off ^a	0.8 nm	NA	
Long range cut-off	1.4 nm	1.4 nm	
System size (# of lipids)	128	512	
Sampling time	120 ns	300 ns	
# replicas	2	1	

Table 10: Table of the changes occurred between simulations run in Poger et al. [16, 15] and the present work, in terms of parameters used and simulation conditions. ^a Settings not reproducible with GROMACS version 2016.3 used in the present work.

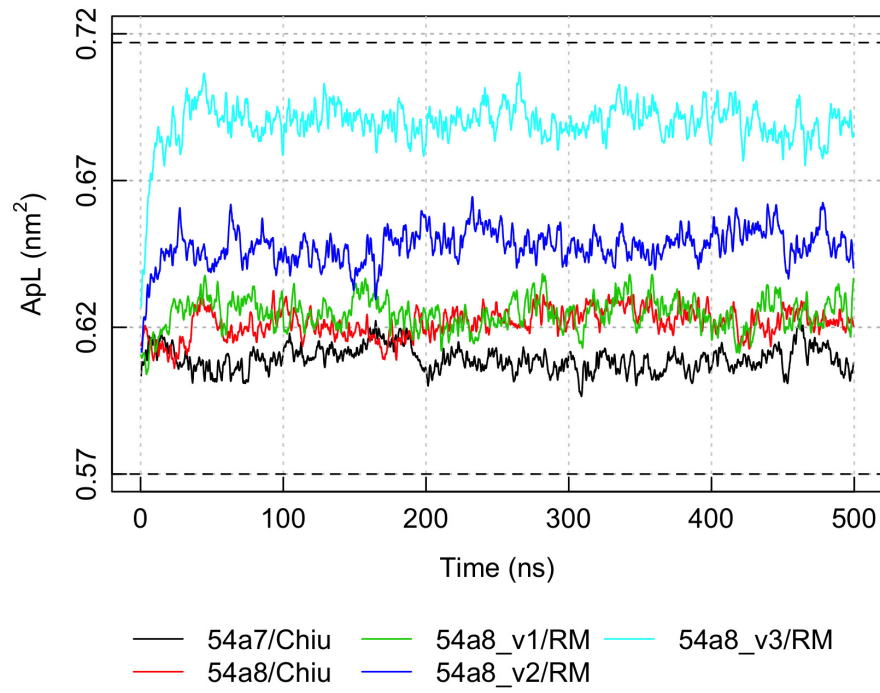


Figure 2: Time series of the area per lipid for a DPPC bilayer, for simulation ID 1 to 5 (see Table 1 for details).

Equilibration of simulations: DPPC [323 K]

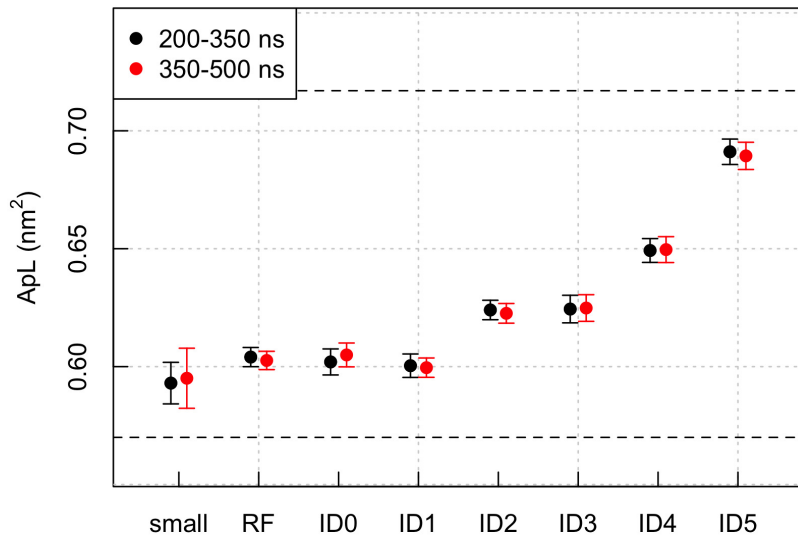


Figure 3: Area per lipid (computed from the simulation box sides) of a DPPC bilayer, for the five test simulation (ID 1 to 5 in Table 1) and the control ones (SI Table 1), computed for two non overlapping time intervals.

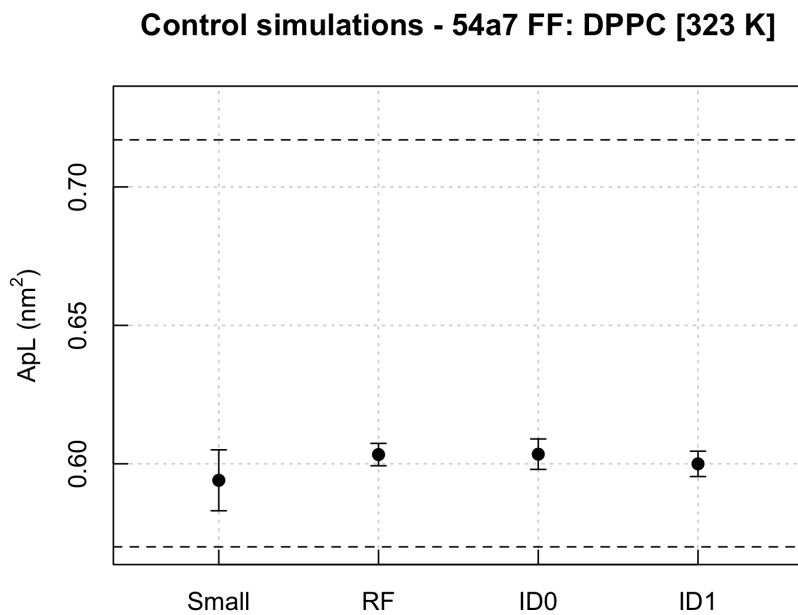


Figure 4: Area per lipid (computed from the simulation box sides) for a DPPC bilayer, for the control simulations as described in SI Table 1). Simulation ID1 (see Table 1) has been included for comparison, as each control simulation (small, RF, ID0) differs from ID1 by only one property (either the system size, long-range electrostatic treatment or the head group partial charges).

DLPC [303 K]

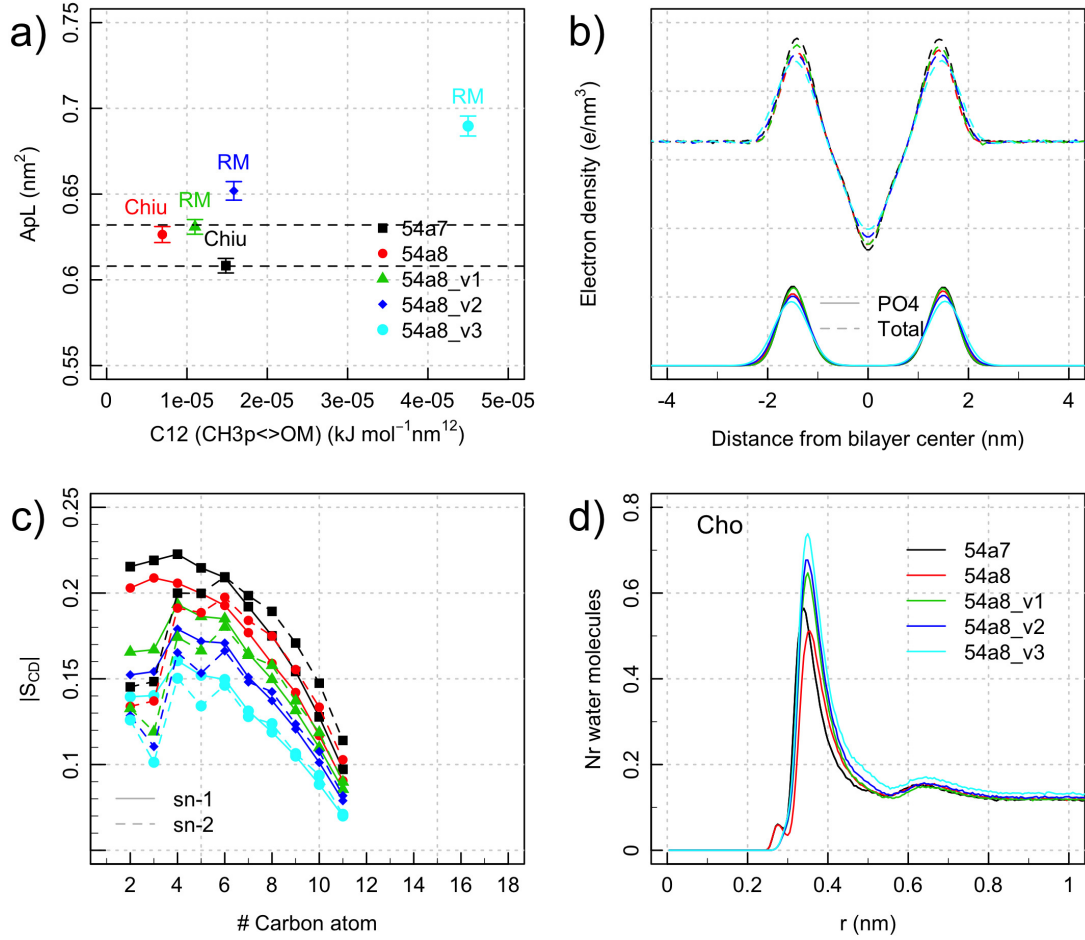


Figure 5: Area per lipid (a), electron density of CH_2 tails and total (b), order parameter (c) and distribution of the distance between water oxygen and the nearest lipid Choline atom for a DLPC bilayer (d), obtained by 5 different sets of parameters (see legend in panel (a,c) and Table 1).

DMPC [303 K]

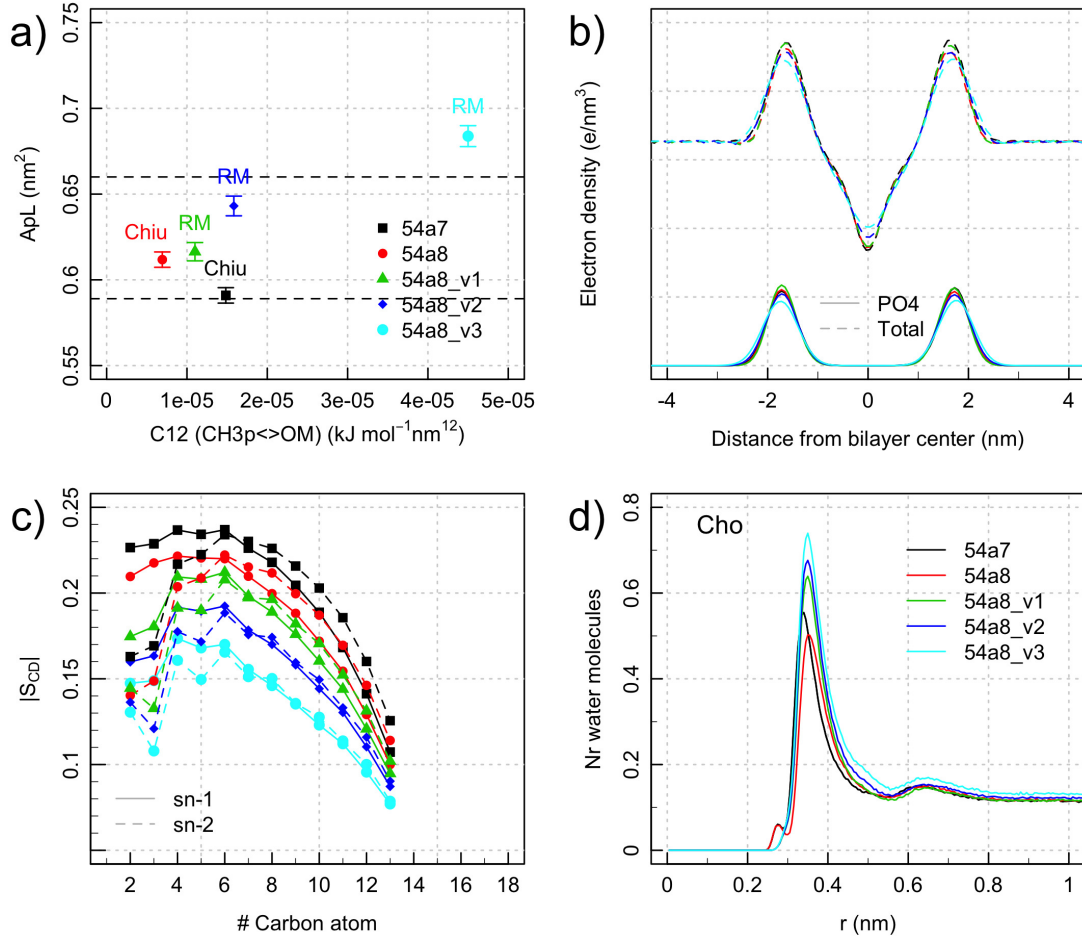


Figure 6: Area per lipid (a), electron density of CH₂ tails and total (b), order parameter (c) and distribution of the distance between water oxygen and the nearest lipid Choline group atom for a DMPC bilayer (d), obtained by 5 different sets of parameters (see legend in panel (a,c) and Table 1).

DOPC [303 K]

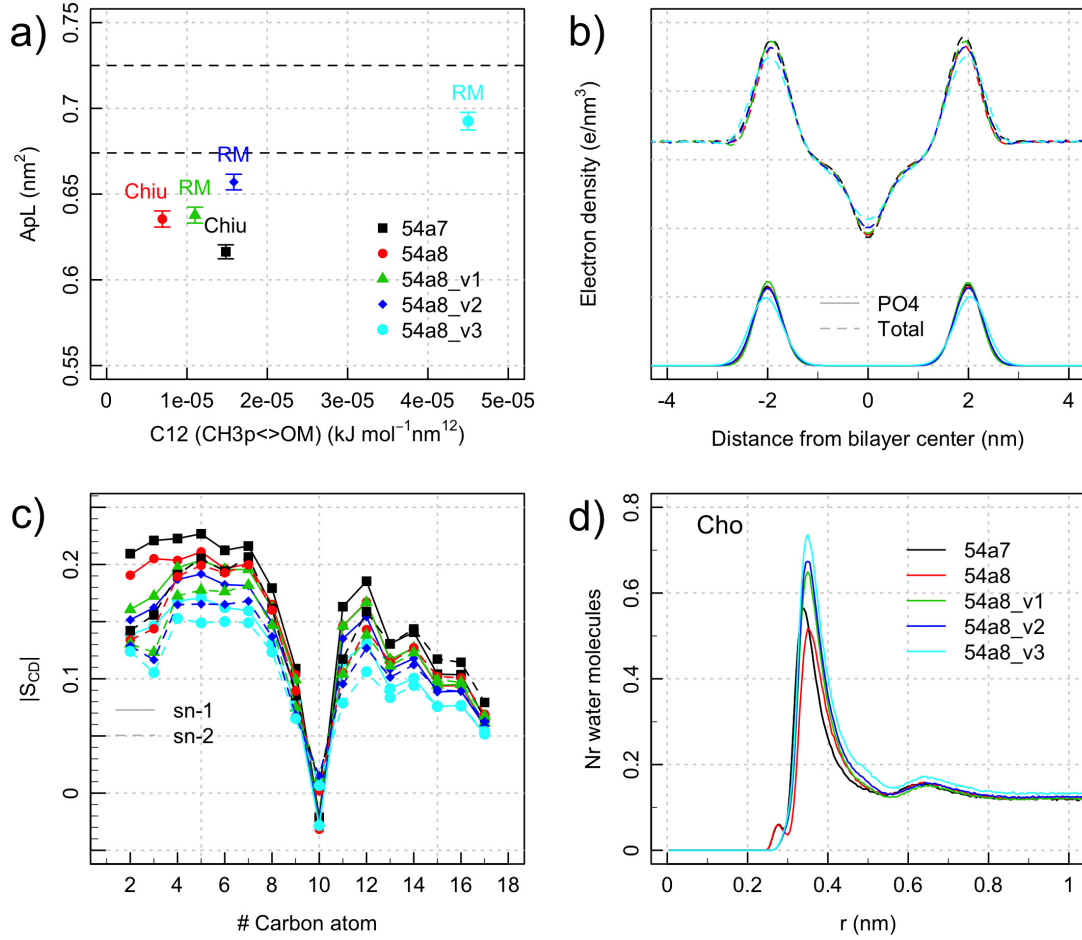


Figure 7: Area per lipid (a), electron density of CH₂ tails and total (b), order parameter (c) and distribution of the distance between water oxygen and the nearest lipid Choline group atom for a DOPC bilayer (d), obtained by 5 different sets of parameters (see legend in panel (a,c) and Table 1).

POPC [323 K]

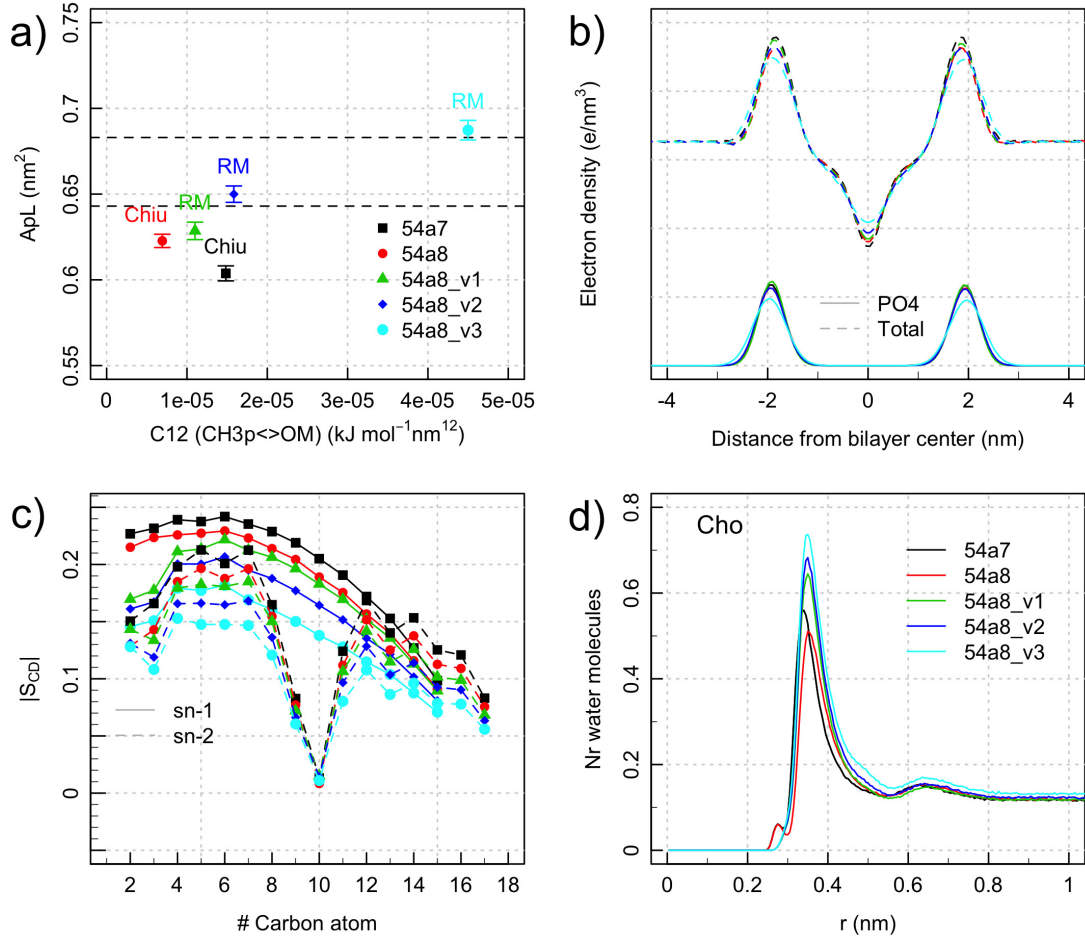


Figure 8: Area per lipid (a), electron density of CH₂ tails and total (b), order parameter (c) and distribution of the distance between water oxygen and the nearest lipid Choline group atom for a POPC bilayer (d), obtained by 5 different sets of parameters (see legend in panel (a,c) and Table 1).

DPPC [303 K]

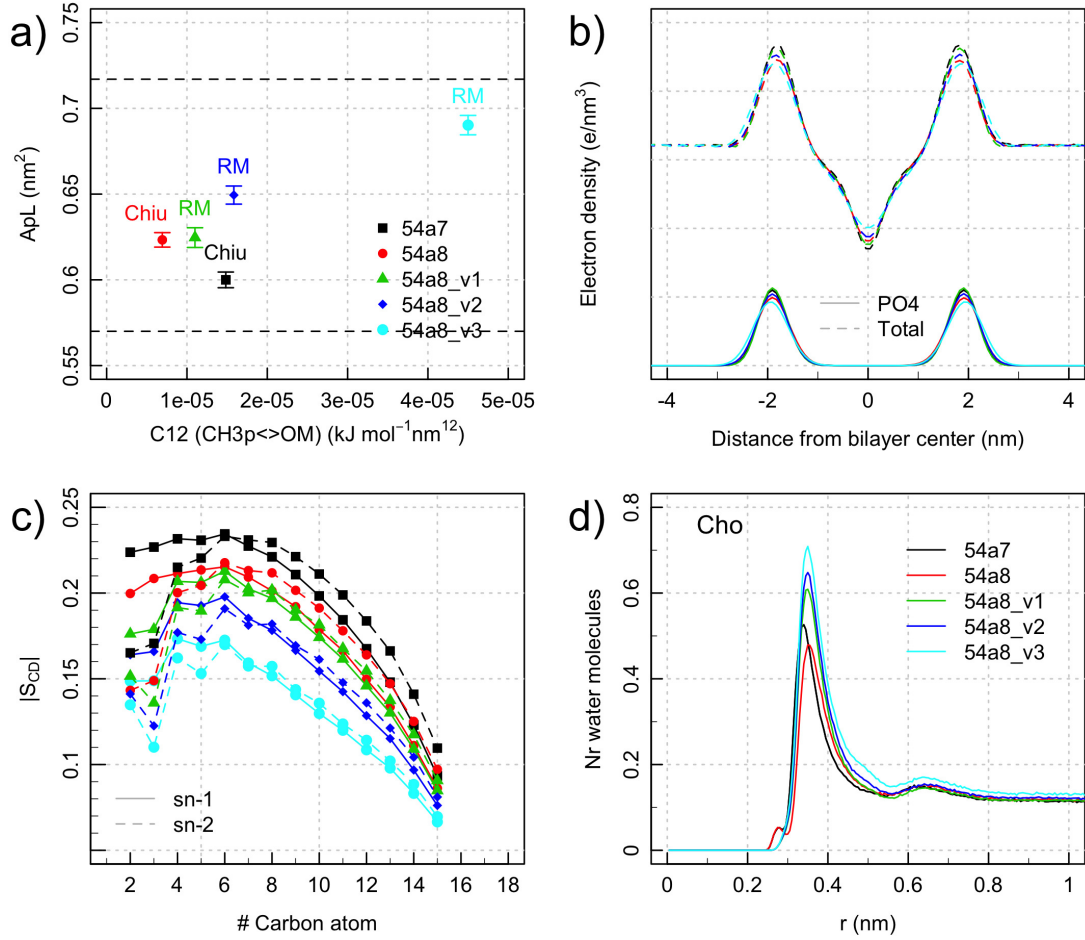


Figure 9: Area per lipid (a), electron density of CH_2 tails and total (b), order parameter (c) and distribution of the distance between water oxygen and the nearest lipid Choline group atom for a DPPC bilayer (d), obtained by 5 different sets of parameters (see legend in panel (a,c) and Table 1).

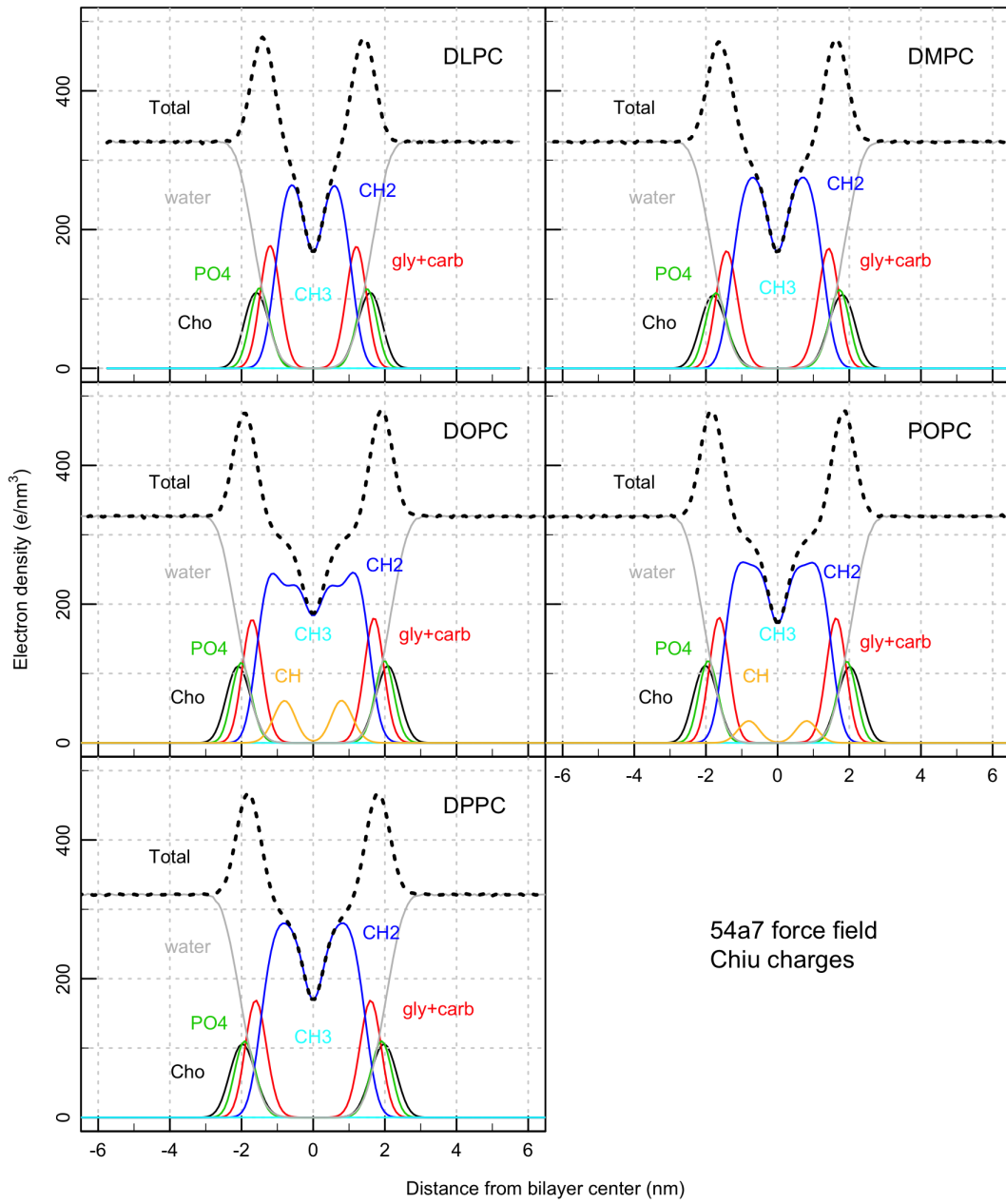


Figure 10: Electron density profiles of the whole hydrated DLPC, DMPC, DOPC, DPPC and POPC bilayers (Total) and of their individual components (Cho: choline, PO4: phosphate, gly+carb: glycerol carbonyl groups, CH2: methylenes of the acyl chains, CH: CHdCH groups in the oleoyl chains, CH3: terminal methyls of the acyl chains) for simulation ID1 (54A7 force field, Chiu charges).

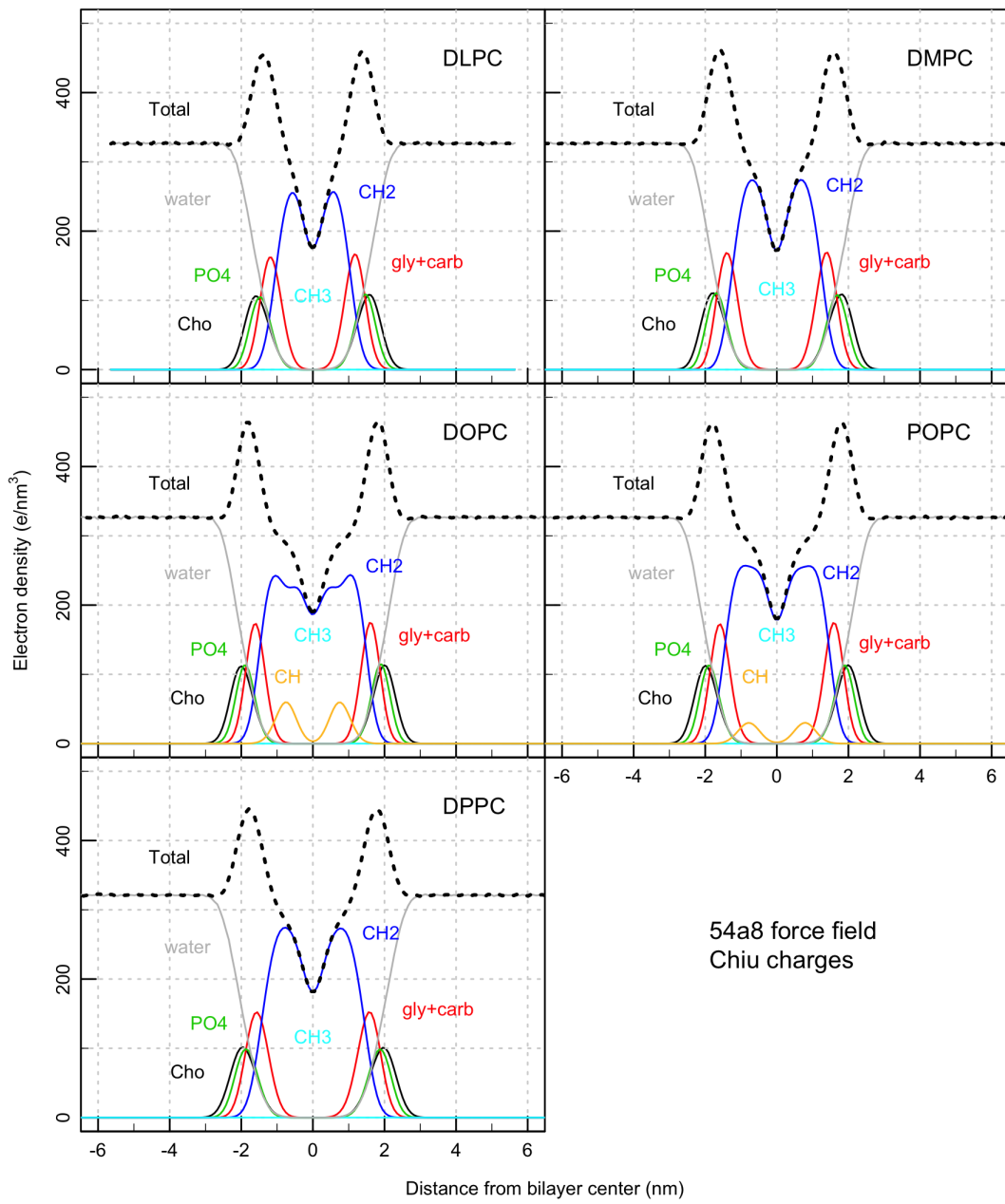


Figure 11: Electron density profiles of the whole hydrated DLPC, DMPC, DOPC, DPPC and POPC bilayers (Total) and of their individual components (Cho: choline, PO4: phosphate, gly+carb: glycerol carbonyl groups, CH2: methylenes of the acyl chains, CH: CHdCH groups in the oleoyl chains, CH3: terminal methyls of the acyl chains) for simulation ID2 (54A8 force field, Chiu charges).

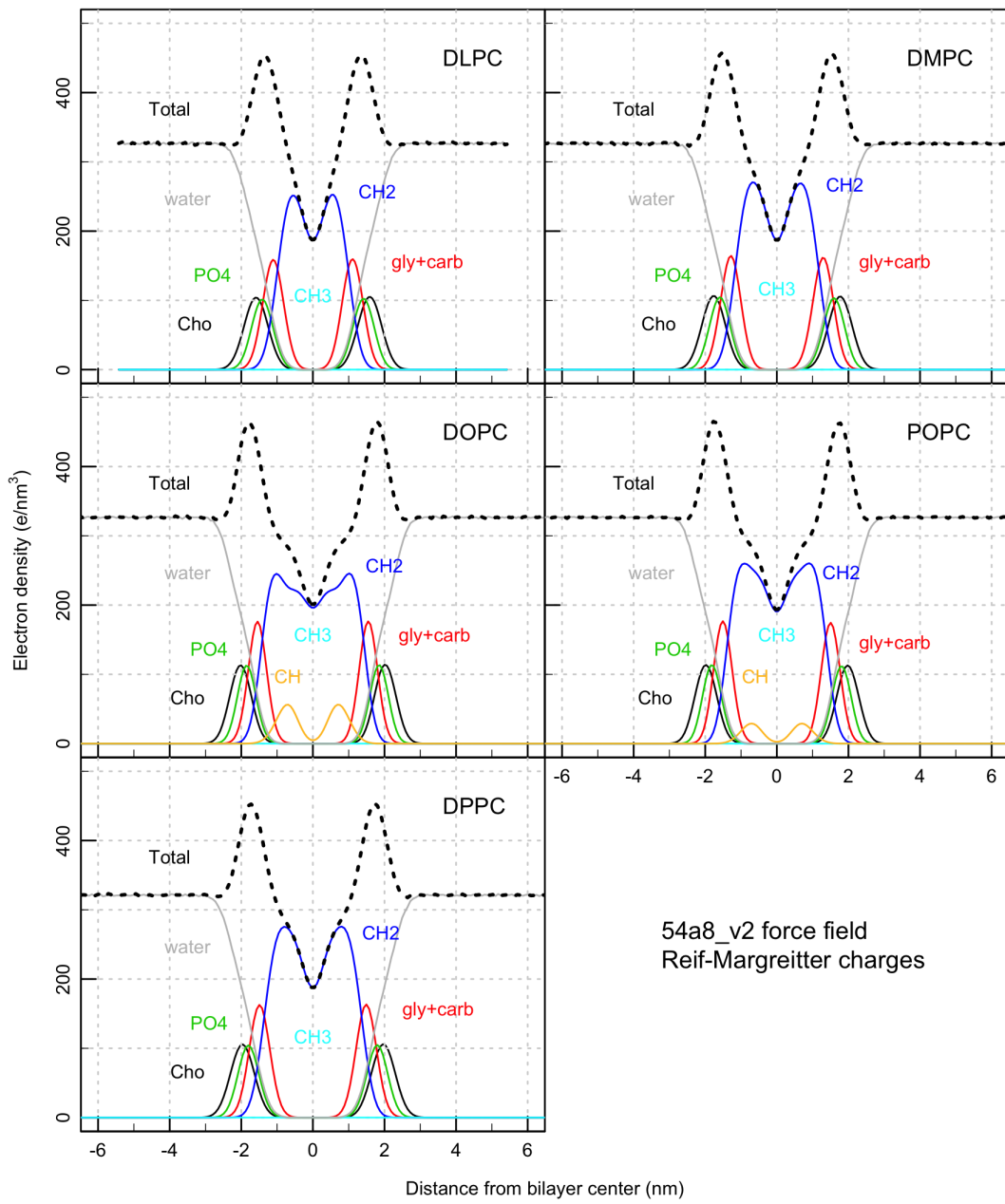


Figure 12: Electron density profiles of the whole hydrated DLPC, DMPC, DOPC, DPPC and POPC bilayers (Total) and of their individual components (Cho: choline, PO4: phosphate, gly+carb: glycerol carbonyl groups, CH2: methylenes of the acyl chains, CH: CHdCH groups in the oleoyl chains, CH3: terminal methyls of the acyl chains) for simulation ID4 (54A8_v2 force field, Reif-Margreitter charges).

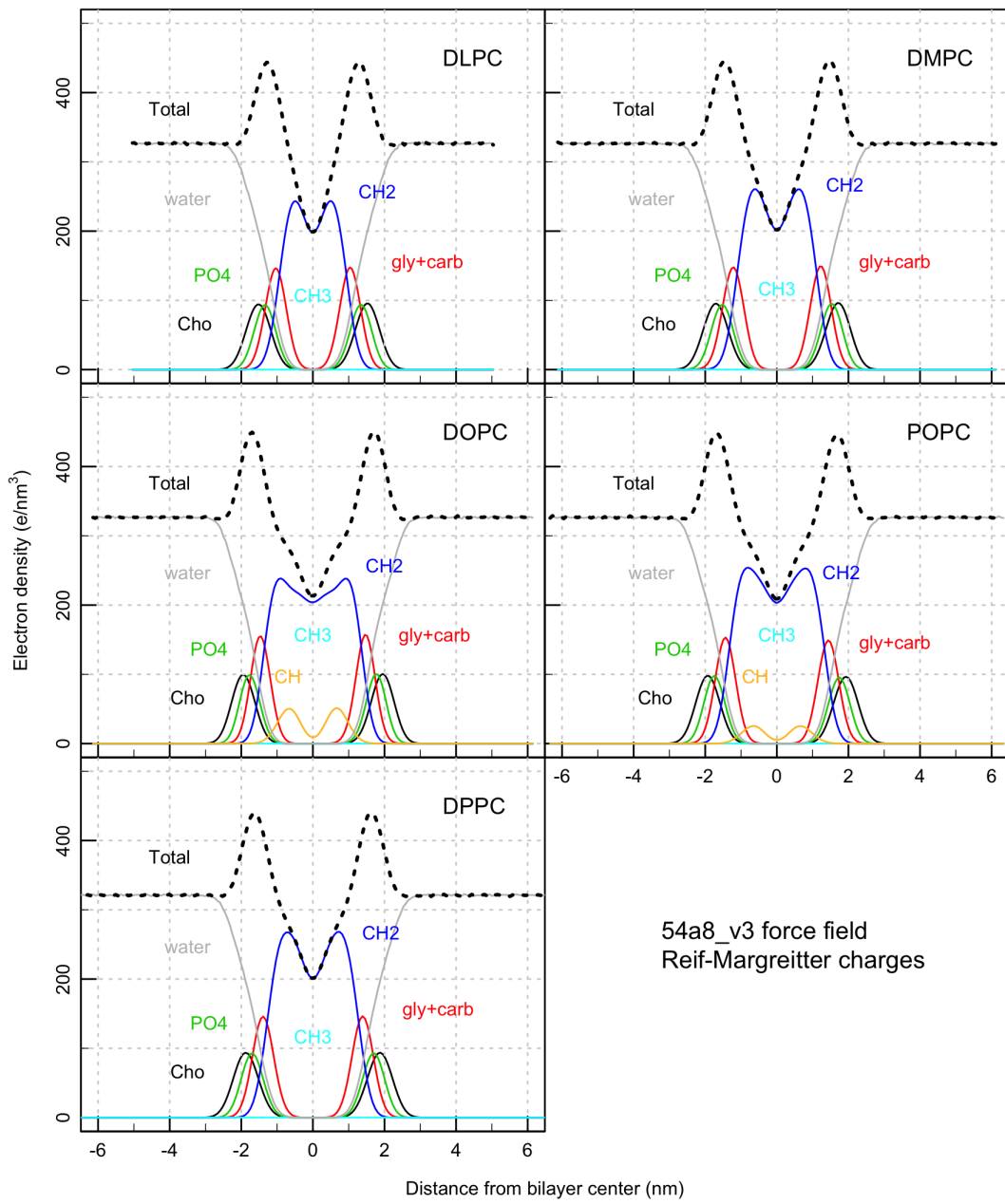


Figure 13: Electron density profiles of the whole hydrated DLPC, DMPC, DOPC, DPPC and POPC bilayers (Total) and of their individual components (Cho: choline, PO4: phosphate, gly+carb: glycerol carbonyl groups, CH2: methylenes of the acyl chains, CH: CHdCH groups in the oleoyl chains, CH3: terminal methyls of the acyl chains) for simulation ID5 (54A8_v3 force field, Reif-Margreitter charges).

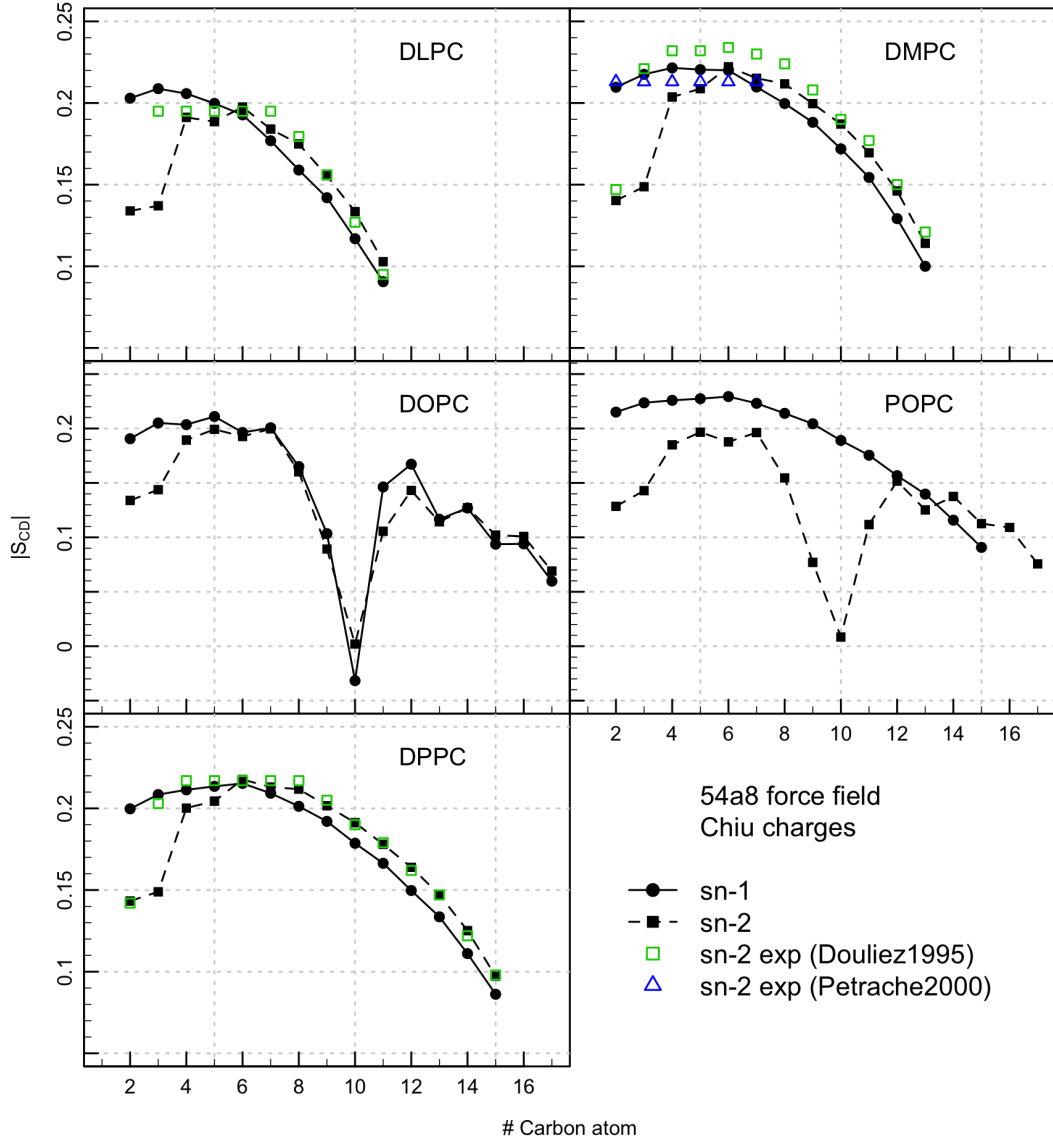


Figure 14: Deuterium order parameter S_{CD} profiles of the sn-1 and sn-2 fatty acyl chains of hydrated DLPC, DMPC, DOPC, DPPC and POPC bilayers calculated from simulations ID2 (54A8 force field, Chiu charges). The S_{CD} values are averaged over all the lipid sn-1 and -2 acyl chains in the systems (proS hydrogen only). Experimental values: Douliez1995 from Ref. [5], Petrache2000 from Ref. [12].

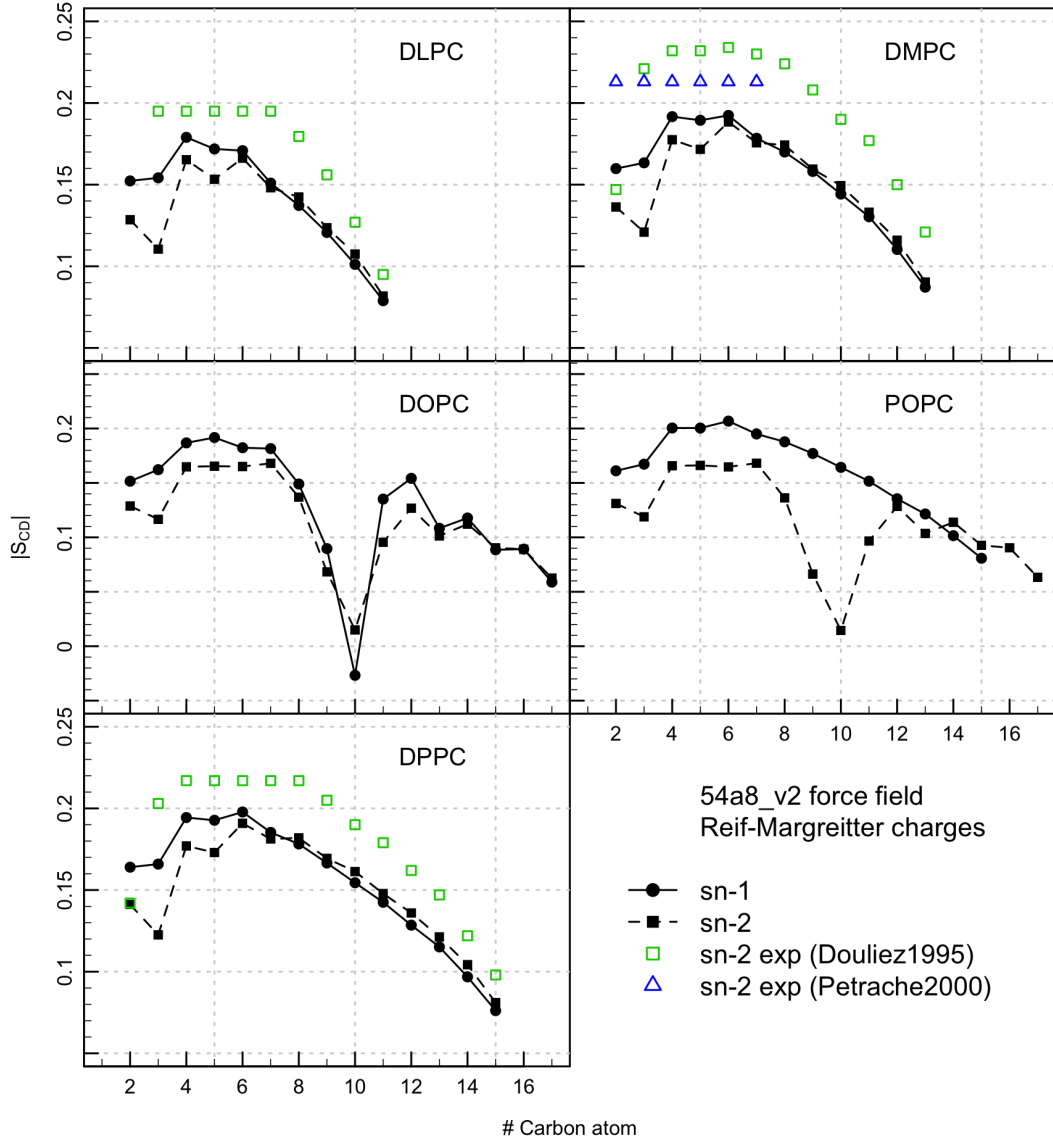


Figure 15: Deuterium order parameter S_{CD} profiles of the sn-1 and sn-2 fatty acyl chains of hydrated DLPC, DMPC, DOPC, DPPC and POPC bilayers calculated from simulations ID4 (54A8_v2 force field, Reif-Margreitter charges). The S_{CD} values are averaged over all the lipid sn-1 and -2 acyl chains in the systems (proS hydrogen only). Experimental values: Douliez1995 from Ref. [5], Petrache2000 from Ref. [12].

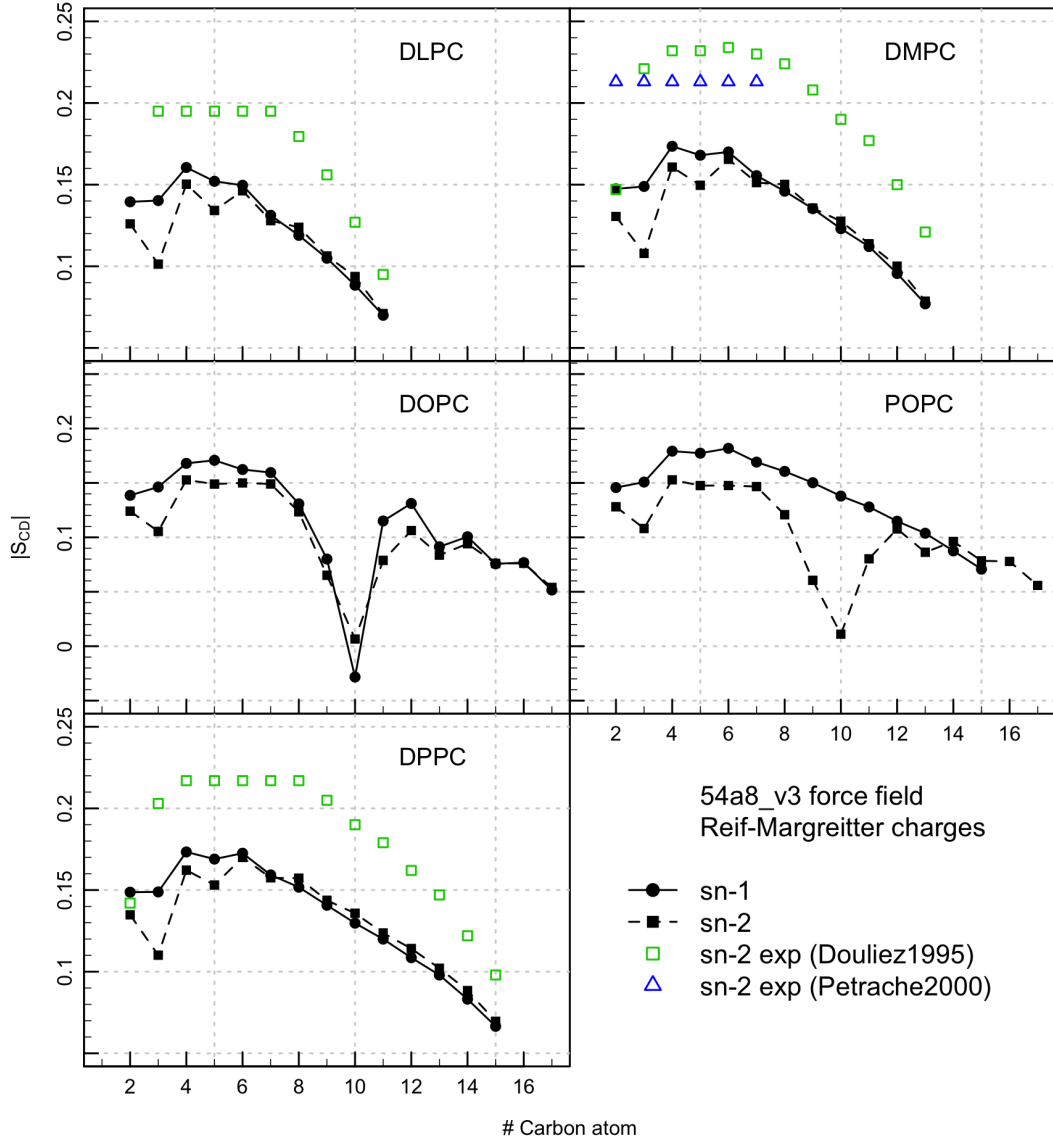


Figure 16: Deuterium order parameter S_{CD} profiles of the sn-1 and sn-2 fatty acyl chains of hydrated DLPC, DMPC, DOPC, DPPC and POPC bilayers calculated from simulations ID5 (54A8_v3 force field, Reif-Margreitter charges). The S_{CD} values are averaged over all the lipid sn-1 and -2 acyl chains in the systems (proS hydrogen only). Experimental values: Douliez1995 from Ref. [5], Petrache2000 from Ref. [12].

DLPC [303 K]

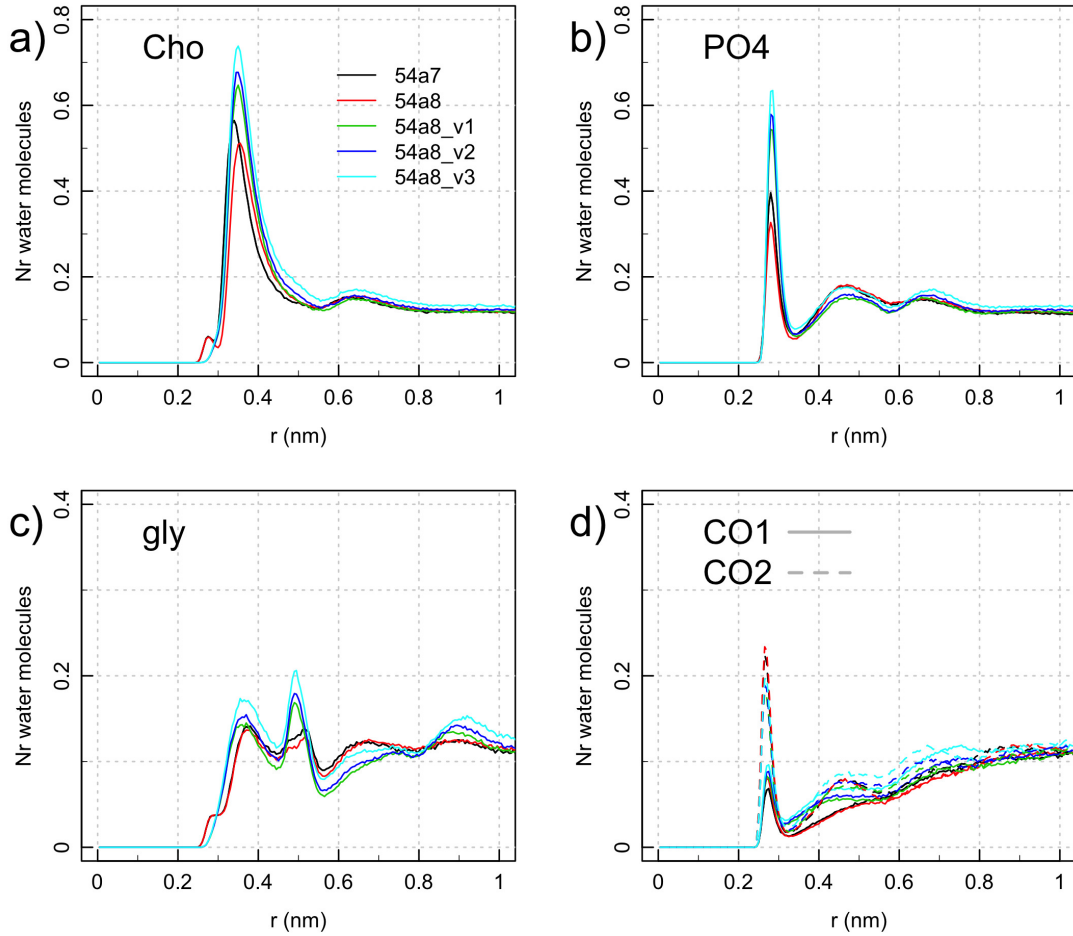


Figure 17: Distribution of the distance between the water oxygen and the nearest lipid head-group atom in given moieties for simulations of a DLPC bilayer. Cho: choline, PO4: phosphate, Gly: glycerol, CO1 and CO2: carbonyl groups at the sn-1 and sn-2 positions.

DMPC [303 K]

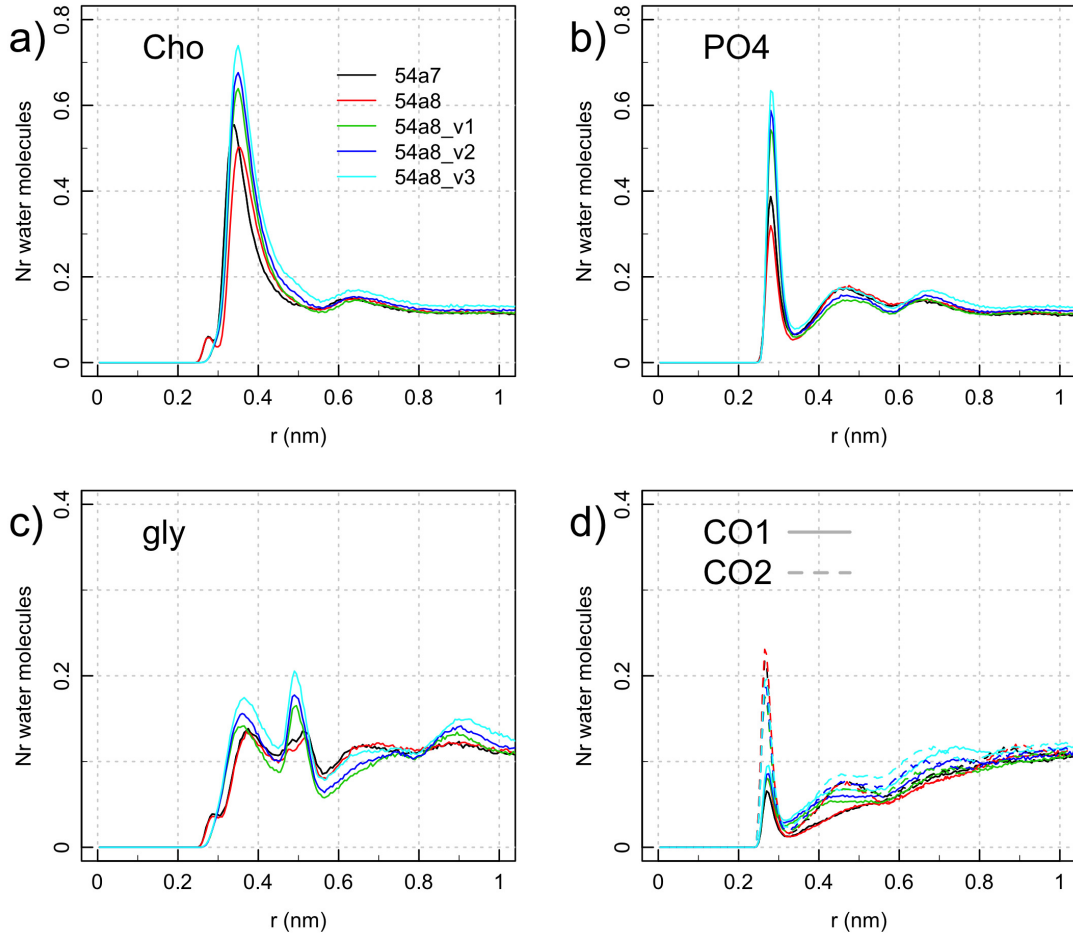


Figure 18: Distribution of the distance between the water oxygen and the nearest lipid head-group atom in given moieties for simulations of a DMPC bilayer. Cho: choline, PO4: phosphate, Gly: glycerol, CO1 and CO2: carbonyl groups at the sn-1 and sn-2 positions.

DOPC [303 K]

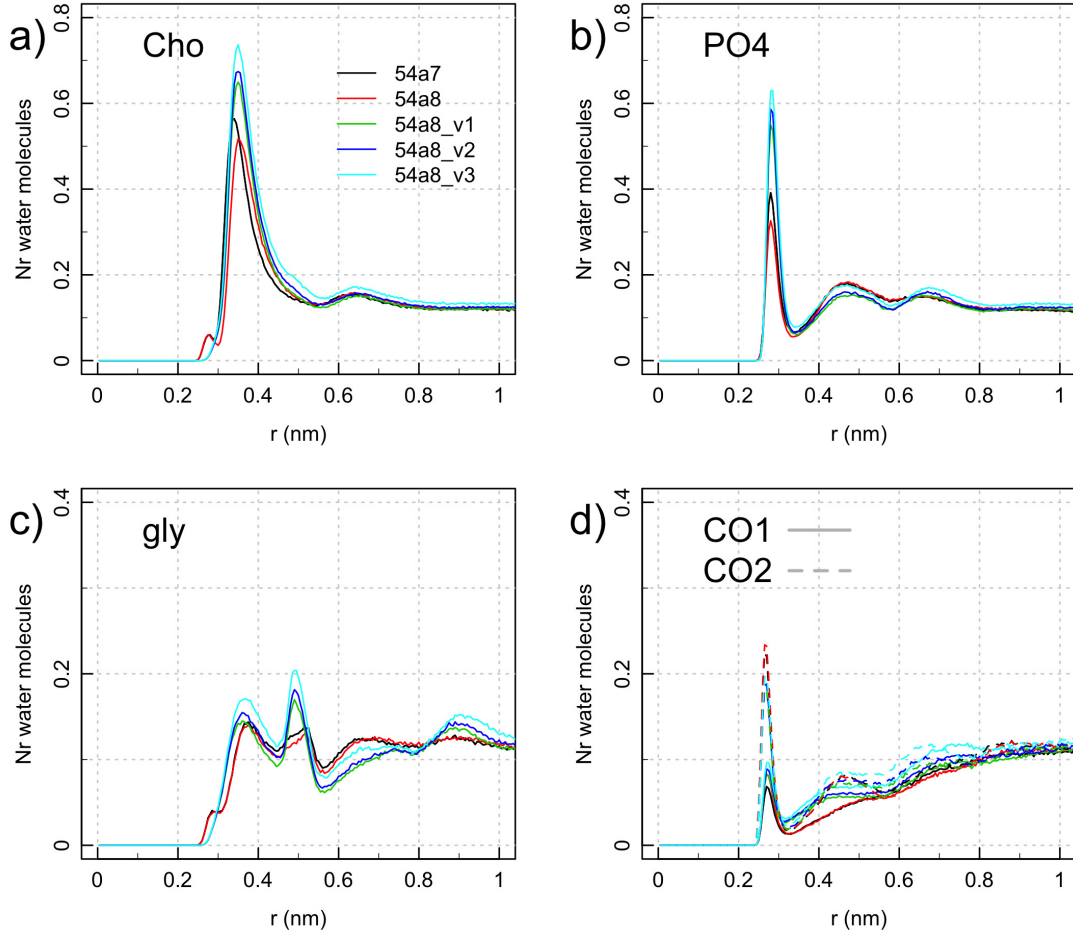


Figure 19: Distribution of the distance between the water oxygen and the nearest lipid head-group atom in given moieties for simulations of a DOPC bilayer. Cho: choline, PO4: phosphate, Gly: glycerol, CO1 and CO2: carbonyl groups at the sn-1 and sn-2 positions.

POPC [323 K]

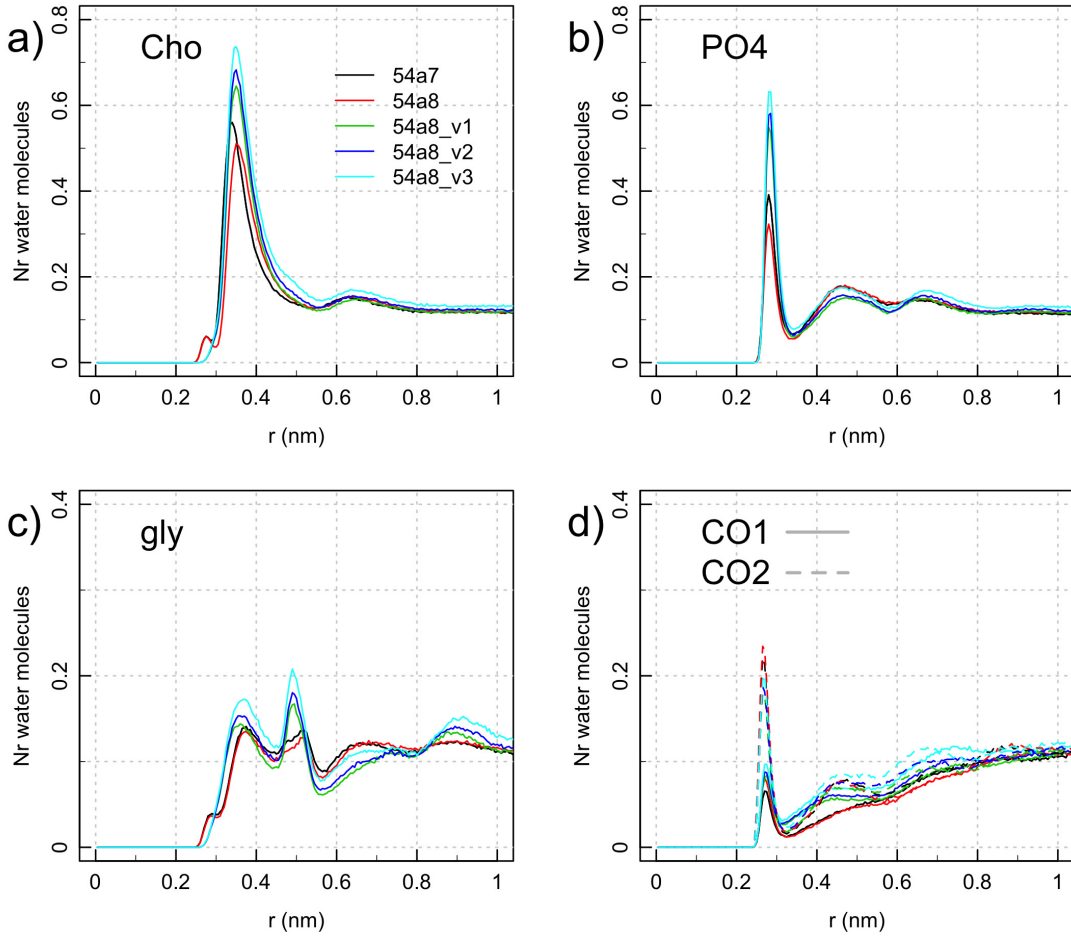


Figure 20: Distribution of the distance between the water oxygen and the nearest lipid head-group atom in given moieties for simulations of a POPC bilayer. Cho: choline, PO4: phosphate, Gly: glycerol, CO1 and CO2: carbonyl groups at the sn-1 and sn-2 positions.

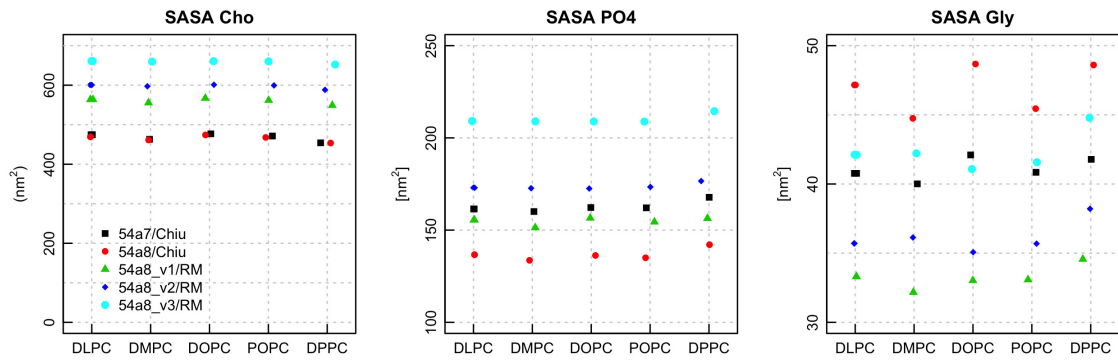


Figure 21: Values of SASA for Choline, Phosphate and Glycerol moieties for all the five phosphocholine and each of the parameter sets simulated.

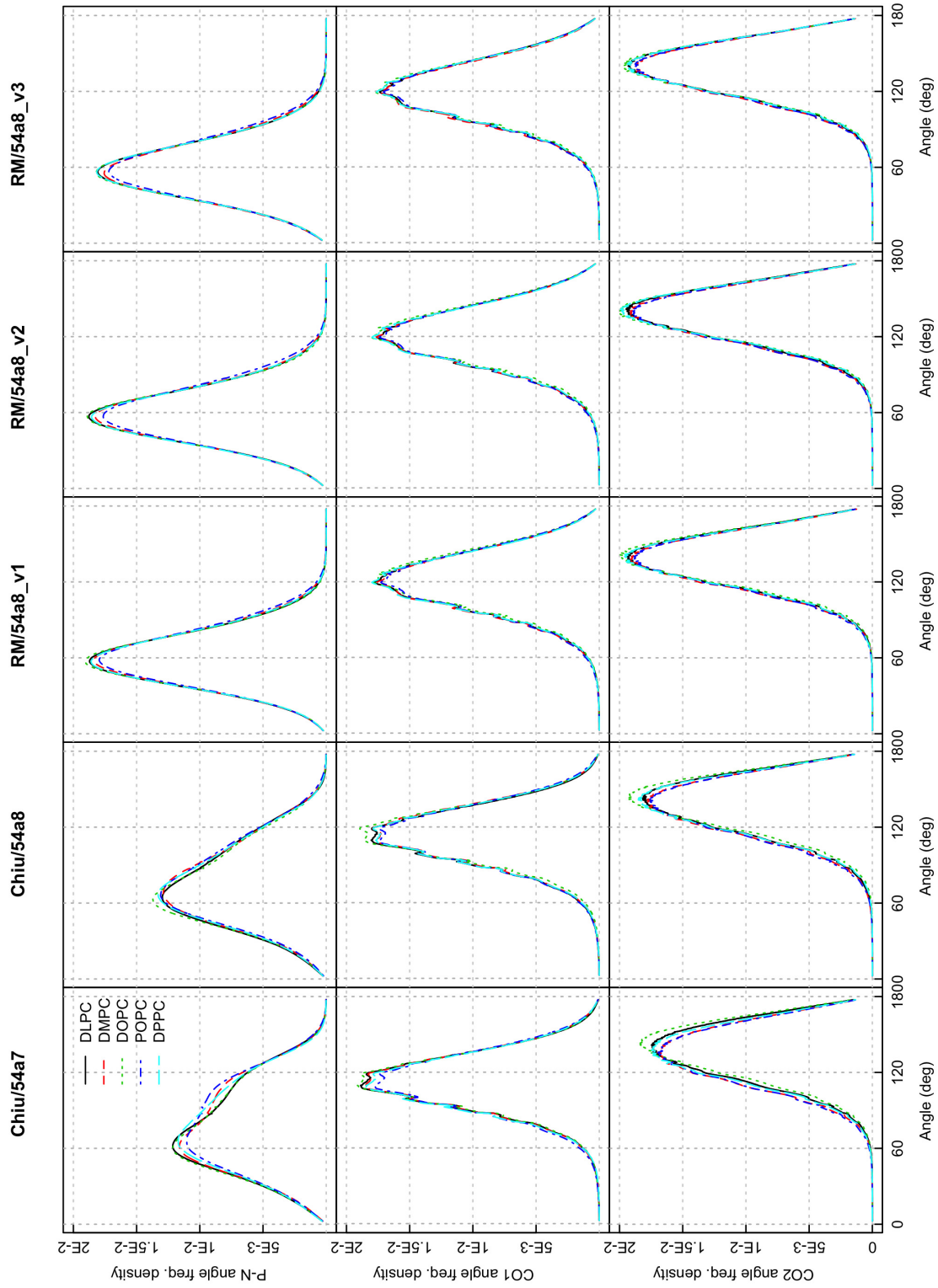


Figure 22: Distribution of the P-N, CO1 and CO2 angles with respect to the outward bilayer normal across different lipids for simulations ID 1 to 5.

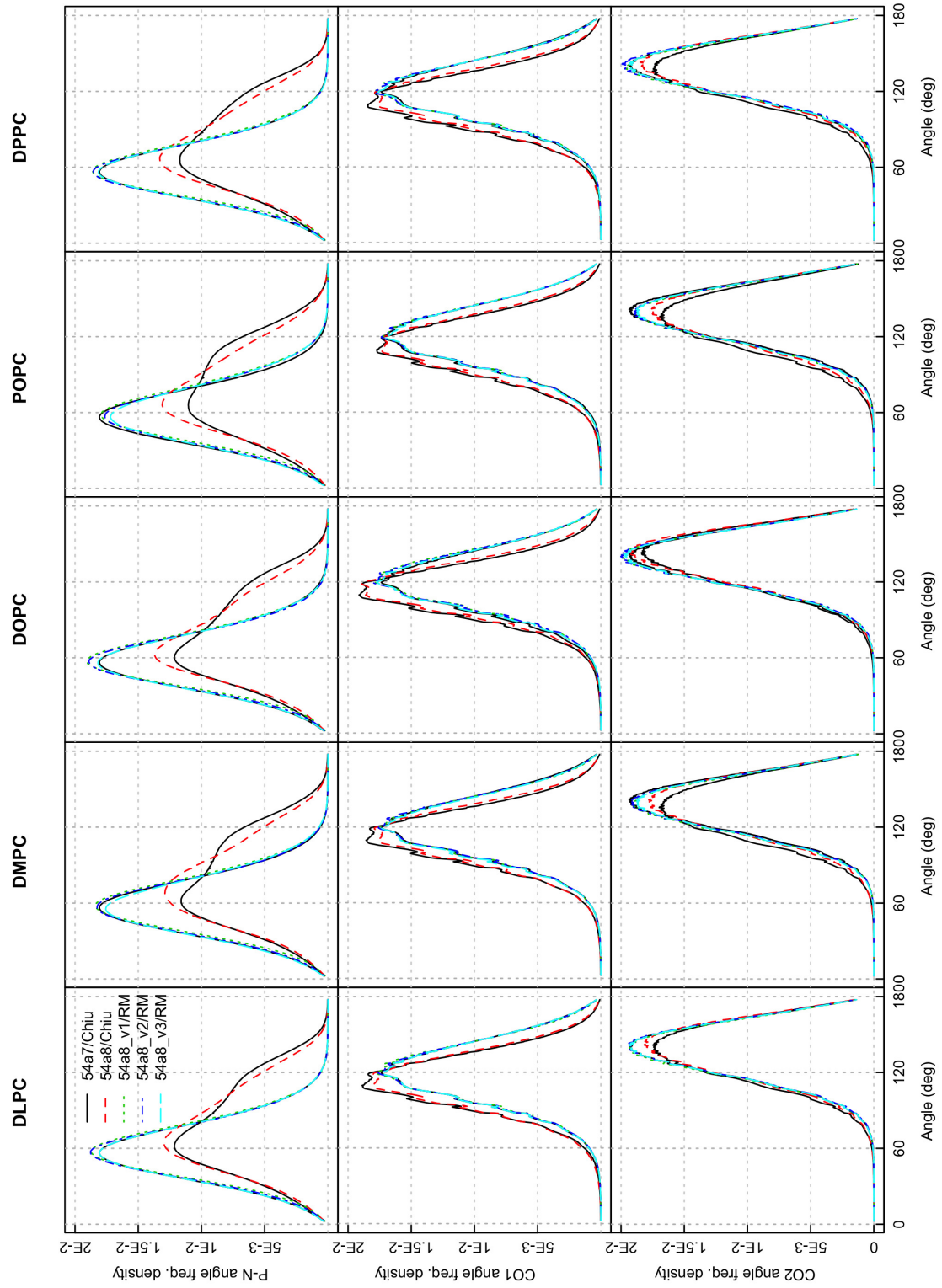


Figure 23: Distribution of the P-N, CO1 and CO2 angles with respect to the outward bilayer normal across different simulations for each lipid.

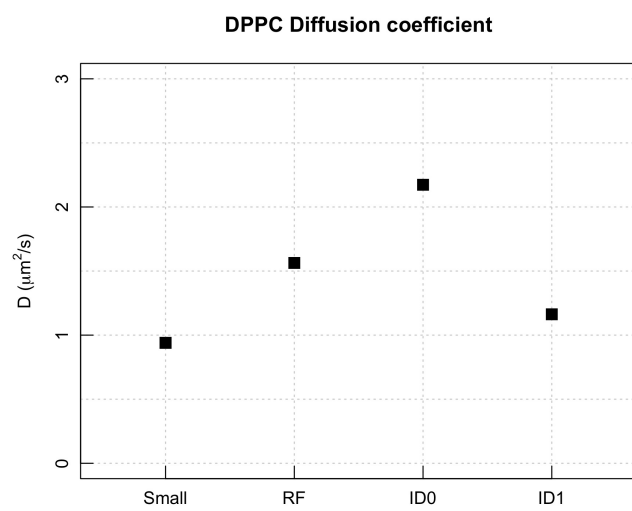


Figure 24: Lateral diffusion coefficient for DPPC in the control simulations as per SI Table 1.

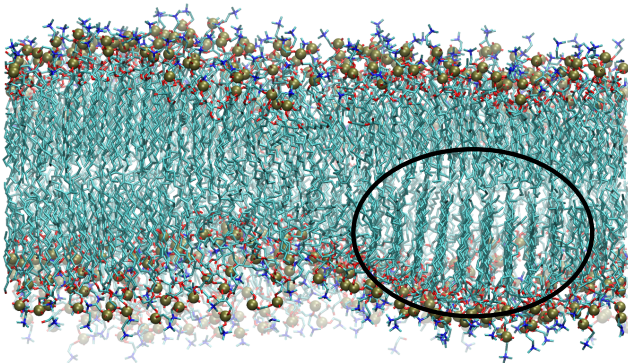


Figure 25: Snapshot after 400 ns simulation of a DPPC patch at 303 K with the 54a8_v1 parameter set. In the circle a detail of the ordered lipid tails which have already transitioned in a gel phase.

POPE [313 K]

54a8/Chiu/CH0

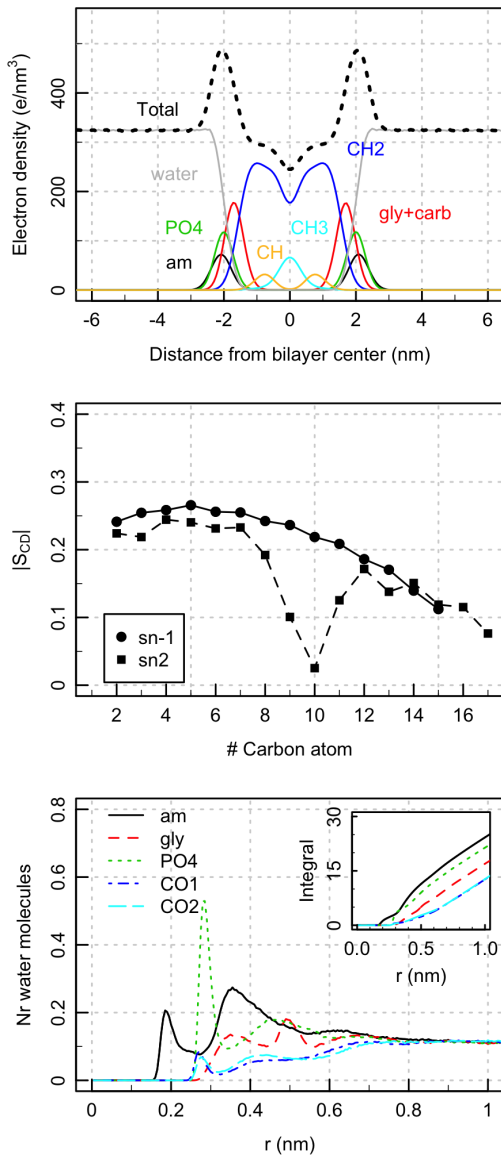


Figure 26: Properties of POPE bilayer simulated with the 54A8 force field, Chiu charges and CH0 esters. Top: electron density profiles (Total: whole bilayer, am: amine, PO4: phosphate, gly+carb: glycerol carbonyl groups, CH2: methylenes of acyl chains, CH: CHdCH groups of oleoyl chains, CH3: terminal methyls); middle: deuterium order parameter S_{CD} of the sn-1 and sn-2 fatty acyl chains (proS hydrogen only); bottom: distribution of the distance between the water oxygen and the nearest lipid headgroup atom - insets: integral of the distribution (am: amine, PO4: phosphate, gly: glycerol, CO1 and CO2: carbonyl groups at the sn-1 and sn-2 positions).

POPE [313 K]

54a8/RM/CH0

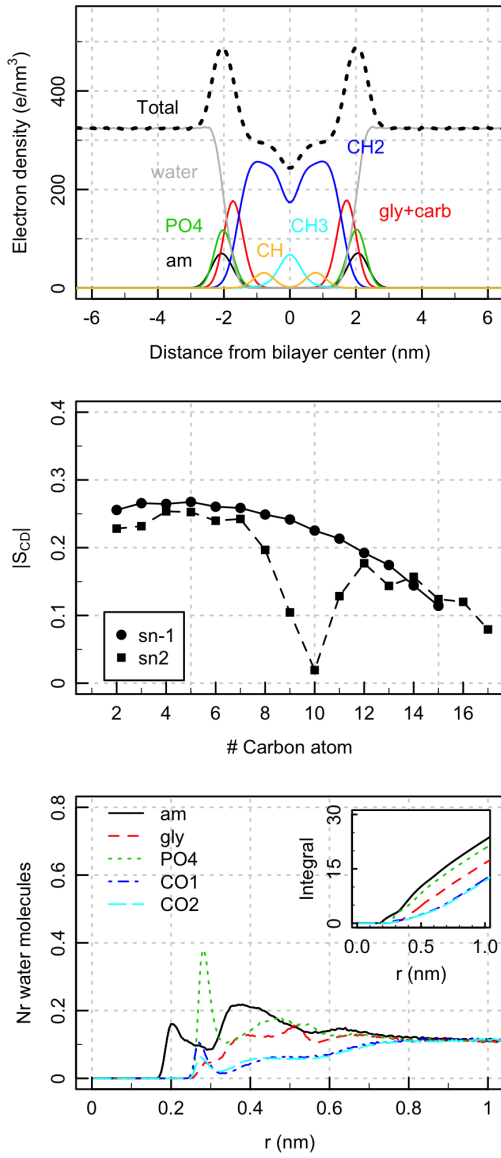


Figure 27: Properties of POPE bilayer simulated with the 54A8 force field, RM charges and CH0 esters. Top: electron density profiles (Total whole bilayer, am amide, PO4 phosphate, gly+carb glycerol carbonyl groups, CH2 methylenes of acyl chains, CH CHdCH groups of oleoyl chains, CH3 terminal methyls); middle: deuterium order parameter S_{CD} of the sn-1 and sn-2 fatty acyl chains (proS hydrogen only); bottom: distribution of the distance between the water oxygen and the nearest lipid headgroup atom - insets: integral of the distribution (am: amine, PO4: phosphate, gly: glycerol, CO1 and CO2: carbonyl groups at the sn-1 and sn-2 positions).

POPG [303 K]

54a8/RM/CH0

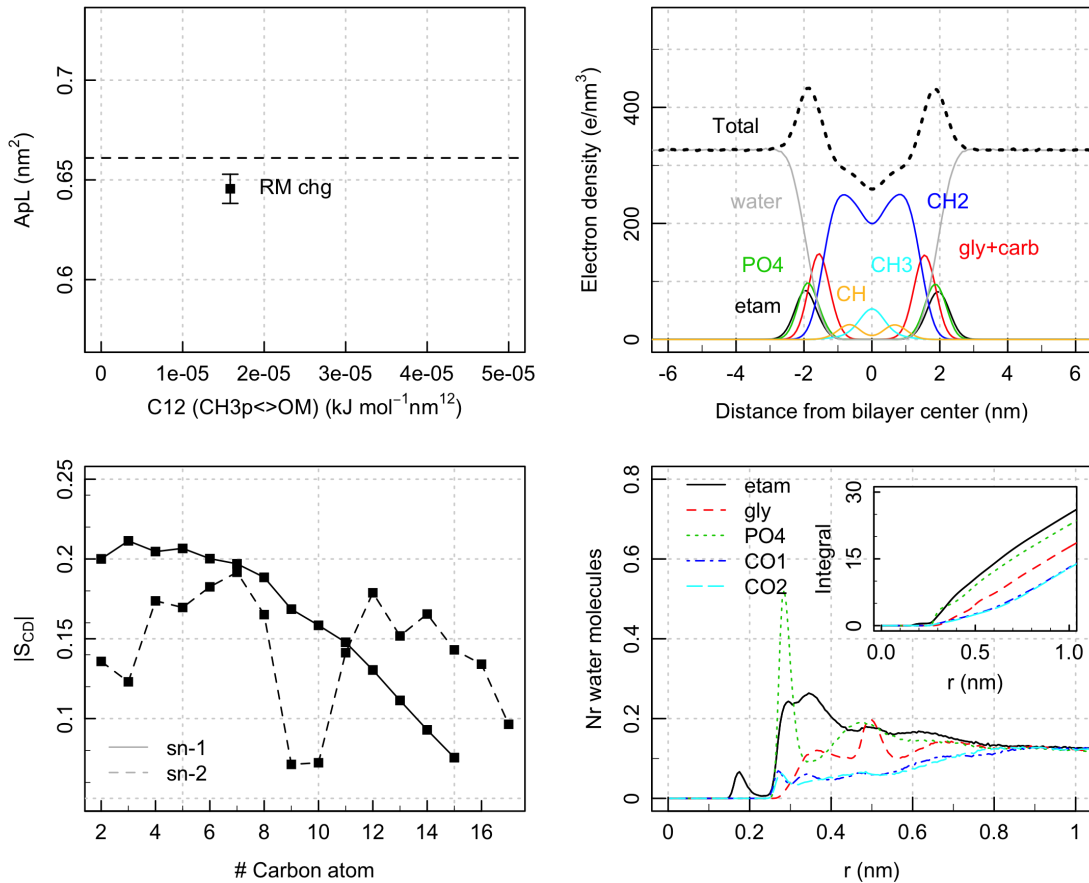


Figure 28: Properties of POPG bilayer simulated with the 54A8 force field, RM charges and CH0 esters. Top left: area per lipid and experimental value (dashed line); top right: electron density profiles (Total: whole bilayer, etam: etamine, PO4: phosphate, gly+carb: glycerol carbonyl groups, CH2: methylenes of acyl chains, CH: CHdCH groups of oleoyl chains, CH3: terminal methyls); bottom left: deuterium order parameter S_{CD} of the sn-1 and sn-2 fatty acyl chains (proS hydrogen only); bottom right: distribution of the distance between the water oxygen and the nearest lipid headgroup atom - insets: integral of the distribution (etam: etamine, PO4: phosphate, gly: glycerol, CO1 and CO2: carbonyl groups at the sn-1 and sn-2 positions).

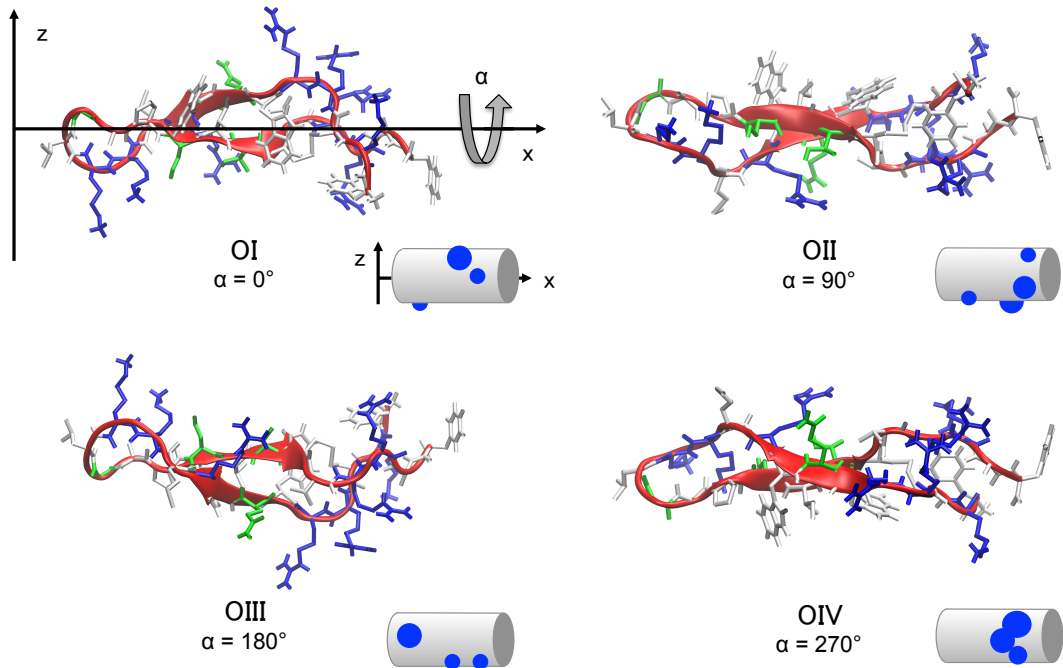


Figure 29: Four different orientations of the peptide 1LFC (bovine lactoferricin) used to sample different initial conditions for the peptide-membrane simulations. OII, OIII and OIV are obtained from OI with an anticlockwise rotation along the main axis (shown as x-axis in OI) of respectively 90° , 180° , 270° . The membrane plane is placed parallel to the main axis of 1LFC; the residues displayed in the bottom are the ones facing the lipids. Backbone red cartoon representation and whole peptide bonds representation coloured by residue type. The insets shows a cartoon representation of the portion of LFC facing the membrane, with blue dots showing the positive patches.

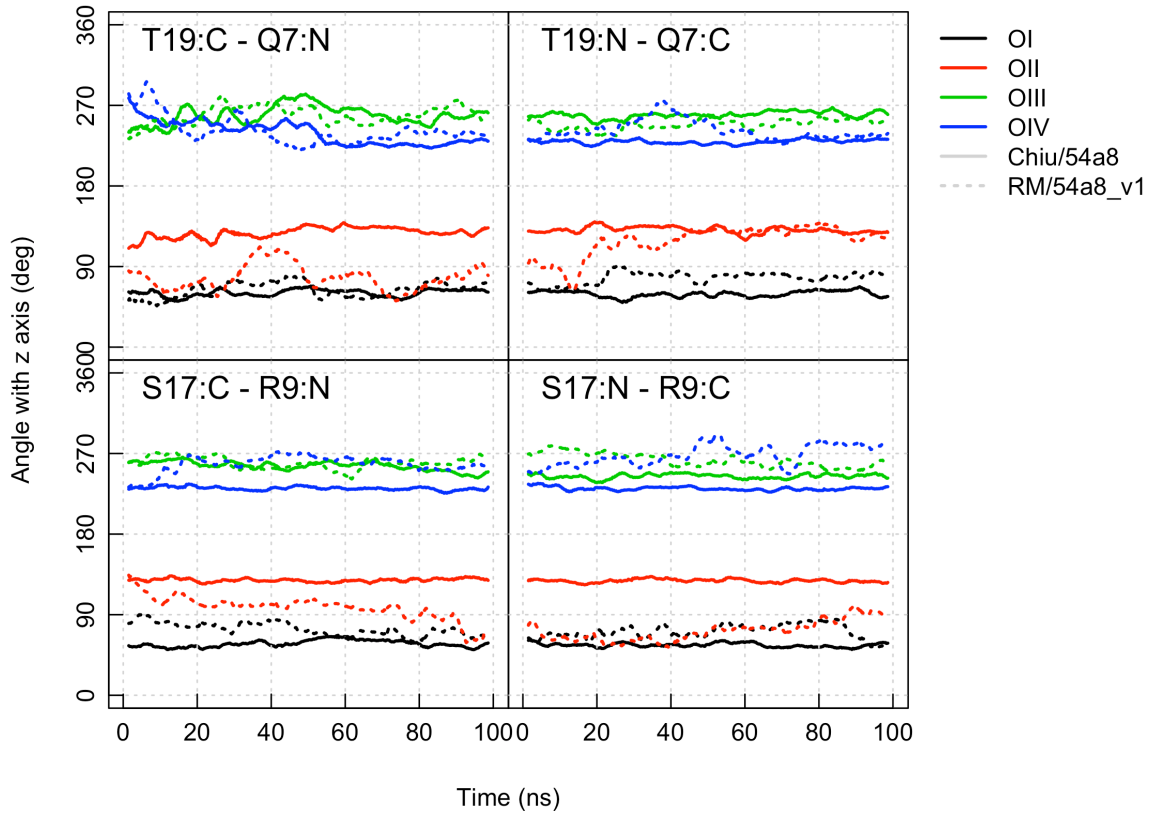


Figure 30: Angle with respect to the z-axis formed by the β -sheet plane. The backbone of amino acids 19 and 17 form hydrogen bonds with the backbone of amino acids 7 and 9 respectively. The vectors connecting the heavy atoms bonded to the O-H pairs forming them are taken as reference to compute the orientation. Solid lines refer to parameter set Chiu/54a8 and dashed ones to set RM/54a8_v1.

References

- [1] M J Abraham et al. *GROMACS User Manual version 2016*. www.gromacs.org, 2018.
- [2] S.-W. Chiu et al. “Incorporation of surface tension into molecular dynamics simulation of an interface: a fluid phase lipid bilayer membrane.” In: *Biophysical journal* 69.4 (1995), pp. 1230–45. ISSN: 0006-3495. DOI: [10.1016/S0006-3495\(95\)80005-6](https://doi.org/10.1016/S0006-3495(95)80005-6).
- [3] R J Clarke. “The dipole potential of phospholipid membranes and methods for its detection”. In: *Advances in Colloid and Interface Science* 89-90 (2001), pp. 263–281. ISSN: 0001-8686. DOI: [10.1016/S0001-8686\(00\)00061-0](https://doi.org/10.1016/S0001-8686(00)00061-0).
- [4] W Ding et al. “Effects of Lipid Composition on Bilayer Membranes Quantified by All-Atom Molecular Dynamics”. In: *The Journal of Physical Chemistry B* 119.49 (2015), pp. 15263–15274. ISSN: 1520-6106. DOI: [10.1021/acs.jpcb.5b06604](https://doi.org/10.1021/acs.jpcb.5b06604).
- [5] J P Douliez, A Léonard, and E J Dufourc. “Restatement of order parameters in biomembranes: calculation of C-C bond order parameters from C-D quadrupolar splittings.” In: *Biophysical journal* 68.5 (1995), pp. 1727–39. ISSN: 0006-3495. DOI: [10.1016/S0006-3495\(95\)80350-4](https://doi.org/10.1016/S0006-3495(95)80350-4).
- [6] U Essmann et al. “A smooth particle mesh Ewald method”. In: *The Journal of Chemical Physics* 103.19 (1995), pp. 8577–8593. ISSN: 0021-9606. DOI: [10.1063/1.470117](https://doi.org/10.1063/1.470117).
- [7] A A Gurtovenko and I Vattulainen. “Calculation of the electrostatic potential of lipid bilayers from molecular dynamics simulations: Methodological issues”. In: *The Journal of Chemical Physics* 130.21 (2009), p. 215107. ISSN: 0021-9606. DOI: [10.1063/1.3148885](https://doi.org/10.1063/1.3148885).
- [8] C Margreitter, M M Reif, and C Oostenbrink. “Update on phosphate and charged post-translationally modified amino acid parameters in the GROMOS force field”. In: *Journal of Computational Chemistry* 38.10 (2017), pp. 714–720. ISSN: 01928651. DOI: [10.1002/jcc.24733](https://doi.org/10.1002/jcc.24733).
- [9] J F Nagle and S Tristram-Nagle. “Structure of lipid bilayers.” In: *Biochimica et biophysica acta* 1469.3 (2000), pp. 159–95. ISSN: 0006-3002.

- [10] C Oostenbrink et al. “A biomolecular force field based on the free enthalpy of hydration and solvation: The GROMOS force-field parameter sets 53A5 and 53A6”. In: *Journal of Computational Chemistry* 25.13 (2004), pp. 1656–1676. ISSN: 1096-987X. DOI: 10.1002/jcc.20090. URL: <http://dx.doi.org/10.1002/jcc.20090>.
- [11] J Pan et al. “Molecular structures of fluid phase phosphatidylglycerol bilayers as determined by small angle neutron and X-ray scattering”. In: *Biochimica et Biophysica Acta (BBA) - Biomembranes* 1818.9 (2012), pp. 2135–2148. ISSN: 00052736. DOI: 10.1016/j.bbamem.2012.05.007.
- [12] H I Petrache, S W Dodd, and M F Brown. “Area per lipid and acyl length distributions in fluid phosphatidylcholines determined by (2)H NMR spectroscopy.” In: *Biophysical journal* 79.6 (2000), pp. 3172–92. ISSN: 0006-3495. DOI: 10.1016/S0006-3495(00)76551-9.
- [13] A D Pickar and R Benz. “Transport of oppositely charged lipophilic probe ions in lipid bilayer membranes having various structures”. In: *The Journal of Membrane Biology* 44.3-4 (1978), pp. 353–376. ISSN: 0022-2631. DOI: 10.1007/BF01944229.
- [14] T J Piggot, D A Holdbrook, and S Khalid. “Electroporation of the E. coli and S. Aureus Membranes: Molecular Dynamics Simulations of Complex Bacterial Membranes”. In: *The Journal of Physical Chemistry B* 115.45 (2011), pp. 13381–13388. ISSN: 1520-6106. DOI: 10.1021/jp207013v.
- [15] D Poger and A E Mark. “On the Validation of Molecular Dynamics Simulations of Saturated and cis -Monounsaturated Phosphatidylcholine Lipid Bilayers: A Comparison with Experiment”. In: *Journal of Chemical Theory and Computation* 6.1 (2010), pp. 325–336. ISSN: 1549-9618. DOI: 10.1021/ct900487a.
- [16] D Poger, W F Van Gunsteren, and A E Mark. “A new force field for simulating phosphatidylcholine bilayers”. In: *Journal of Computational Chemistry* 31.6 (2010), pp. 1117–1125. ISSN: 01928651. DOI: 10.1002/jcc.21396.

- [17] R P Rand et al. “Variation in hydration forces between neutral phospholipid bilayers: evidence for hydration attraction”. In: *Biochemistry* 27.20 (1988), pp. 7711–7722. ISSN: 0006-2960. DOI: [10.1021/bi00420a021](https://doi.org/10.1021/bi00420a021).
- [18] M M Reif, P H Hünenberger, and C Oostenbrink. “New Interaction Parameters for Charged Amino Acid Side Chains in the GROMOS Force Field”. In: *Journal of Chemical Theory and Computation* 8.10 (2012), pp. 3705–3723. ISSN: 1549-9618. DOI: [10.1021/ct300156h](https://doi.org/10.1021/ct300156h).
- [19] J Schamberger and R J Clarke. “Hydrophobic Ion Hydration and the Magnitude of the Dipole Potential”. In: *Biophysical Journal* 82.6 (2002), pp. 3081–3088. ISSN: 0006-3495. DOI: [10.1016/S0006-3495\(02\)75649-X](https://doi.org/10.1016/S0006-3495(02)75649-X).
- [20] T Starke-Peterkovic and R J Clarke. “Effect of headgroup on the dipole potential of phospholipid vesicles”. In: *European Biophysics Journal* 39.1 (2009), pp. 103–110. ISSN: 0175-7571. DOI: [10.1007/s00249-008-0392-y](https://doi.org/10.1007/s00249-008-0392-y).
- [21] I G Tironi et al. “A generalized reaction field method for molecular dynamics simulations”. In: 102.13 (1995), pp. 5451–5459. ISSN: 0021-9606. DOI: [10.1063/1.469273](https://doi.org/10.1063/1.469273).
- [22] L Wang, P S Bose, and F J Sigworth. “Using cryo-EM to measure the dipole potential of a lipid membrane”. In: *Proceedings of the National Academy of Sciences* 103.49 (2006), pp. 18528–18533. ISSN: 0027-8424. DOI: [10.1073/PNAS.0608714103](https://doi.org/10.1073/PNAS.0608714103).
- [23] D T Warshaviak, M J Muellner, and M Chachisvilis. “Effect of membrane tension on the electric field and dipole potential of lipid bilayer membrane”. In: *Biochimica et Biophysica Acta (BBA) - Biomembranes* 1808.10 (2011), pp. 2608–2617. ISSN: 00052736. DOI: [10.1016/j.bbamem.2011.06.010](https://doi.org/10.1016/j.bbamem.2011.06.010).